

Sandia Vertical-Axis Wind Turbine Program Technical Quarterly Report January-March 1976

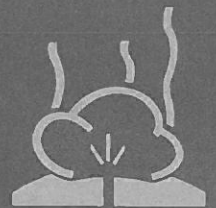
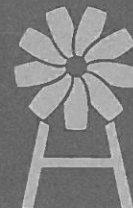
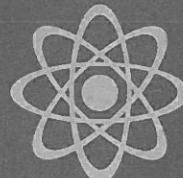
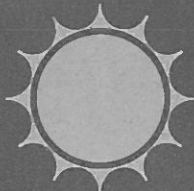
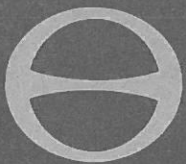
Lawrence I. Weingarten, Ben F. Blackwell

Prepared by Sandia Laboratories, Albuquerque, New Mexico 87115
and Livermore, California 94550 for the United States Energy Research
and Development Administration under Contract AT (29-1)-789

Printed August 1976



Sandia Laboratories
energy report



Issued by Sandia Laboratories, operated for the United States
Department of Energy by Sandia Corporation.

NOTICE

This report was prepared as an account of work sponsored by the United States Government. Neither the United States nor the Department of Energy, nor any of their employees, nor any of their contractors, subcontractors, or their employees, makes any warranty, express or implied, or assumes any legal liability or responsibility for the accuracy, completeness or usefulness of any information, apparatus, product or process disclosed, or represents that its use would not infringe privately owned rights.

SF 1004-DF(11-77)

SAND76-0338
Unlimited Release
Printed August 1976

SANDIA VERTICAL-AXIS WIND TURBINE PROGRAM
TECHNICAL QUARTERLY REPORT
January-March 1976

Advanced Energy Projects Division, 5715

Edited by

Lawrence I. Weingarten
Applied Mechanics Division III, 1284

Ben F. Blackwell
Aerothermodynamics Division, 1333

Sandia Laboratories
Albuquerque, New Mexico 87115

ABSTRACT

This quarterly report describes the activities within the Sandia Laboratories Vertical-Axis Wind Turbine Program during the third quarter of fiscal year 1976. Included are the highlights of the quarter; a review of the status of general design efforts in the areas of aerodynamics, structures, systems analysis, and testing; a summary of preliminary design details of the proposed 17-m turbine/60-kW generator system for power grid application; and structural analysis and operational test results for the existing 5-m turbine.

Printed in the United States of America

Available from
National Technical Information Service
U. S. Department of Commerce
5285 Port Royal Road
Springfield, Virginia 22161
Price: Printed Copy \$5.50; Microfiche \$2.25

ILLUSTRATIONS

<u>Figure</u>		<u>Page</u>
1	Comparison of Theory With Experimental Data, 0.3 Solidity	12
2	Comparison of Theory With Experimental Data, 0.13 Solidity	12
3	Finite Element Model of VAWT With Three Blades, Struts, and Four-Cable Outriggers	14
4	Ratio of the Weight of Tubular and Truss Towers That Have Equivalent Bending Stiffnesses	15
5	Relationship Between Geometries of Tubular and Truss Towers That Have Equivalent Bending Stiffnesses	16
6	Model Power Coefficient	17
7	Energy Per Unit Swept Area	18
8	Energy Per Unit Rated Torque	18
9	Power Coefficients From Aerodynamic Model	19
10	Flow Chart of Economics Model	20
11	Reference Cost Case	21
12	Variation of Energy Cost With Solidity	21
13	Variation of Solidity With Chord/Radius	22
14	Variation of Energy Cost With Chord/Radius	22
15	Effects of Component Cost Reductions	23
16	Combined Effects of Potential Cost Reductions	23
17	Combined Effects of Potential Cost Reductions	24
18	Automatic Control of VAWT	25
19	Microprocessor Program Flow Chart for VAWT	26
20	Wind Instrumentation Systems	27
21	Comparison Between Sandia and NRC Experimental Performance Data	27
22	Lift Coefficients for Four Airfoil Sections at Reynolds No. $\cong 0.7 \times 10^6$	29
23	Wind Turbine Blade Geometry	32
24	Kaman Blade Cross Section	32
25	Nonrotating In-Plane Deformation	33
26	Nonrotating In-Plane Deformation With Severe Gust	33
27	Isometric View of VAWT. Example of Out-of-Plane Blade Mode Shape	36
28	Isometric View of VAWT. Example of In-Plane Blade Mode Shape	36
29	Isometric View of VAWT. Example of Tower Bending Influenced Mode Shape	37

ILLUSTRATIONS (cont)

<u>Figure</u>		<u>Page</u>
30	Ratio of the Weights of Tubular and Truss Towers Which Have Equivalent Torsional Stiffnesses	38
31	Relationship Between the Geometries of Tubular and Truss Tower Which Have Equivalent Torsional Stiffnesses	39
32	Minimum Weight Design Curves for Tubular Towers	39
33	Turbine Base Design Schematic	40
34	Pointwise Torque and Velocity Data (175-rpm) Sampled at 0.5-Second Intervals. Circular Points Are for 5-Second Averages	45
35	Five-Second Averaged Data. Approximately 3 Minutes of Data (175-rpm)	45
36	Repeatability Test. Same Configuration as Figure 35 With a Different Windspeed Record	46
37	Method of Bins, Showing the Velocity Distribution (upper points) and Torque vs. Velocity for 175-rpm Operations	47
38	Method of Bins With an Expanded Velocity Distribution for 150-rpm Operations	48
39	Families of Torque vs. Windspeed Responses Showing the Effect of rpm on Turbine Output	49
40	Power Coefficient Calculated From the 150-rpm Data of Figure 38	49

FOREWORD AND ACKNOWLEDGMENTS

The work covered herein was performed by Sandia Laboratories under a contract administered by the Wind Energy Conversion Branch (Division of Solar Energy) of the Energy Research and Development Administration. The time period is January 1, 1976, to March 31, 1976. Previous work was reported in Sandia Vertical-Axis Wind Turbine Program Technical Quarterly Report, October-December 1975, SAND76-0036, printed April 1976.

The report represents contributions from the following Sandia staff members:

J. F. Banas	R. C. Reuter
J. H. Biffle	R. Rodeman
B. F. Blackwell	R. E. Sheldahl
L. V. Feltz	W. N. Sullivan
R. D. Grover	A. F. Veneruso
E. G. Kadlec	L. I. Weingarten
D. W. Lobitz	

The following Sandia personnel contributed significantly to the hardware development aspects of the program:

- K. G. Grant
- C. E. Longfellow
- R. S. Rusk
- J. Lackey
- R. Anderson

SUMMARY

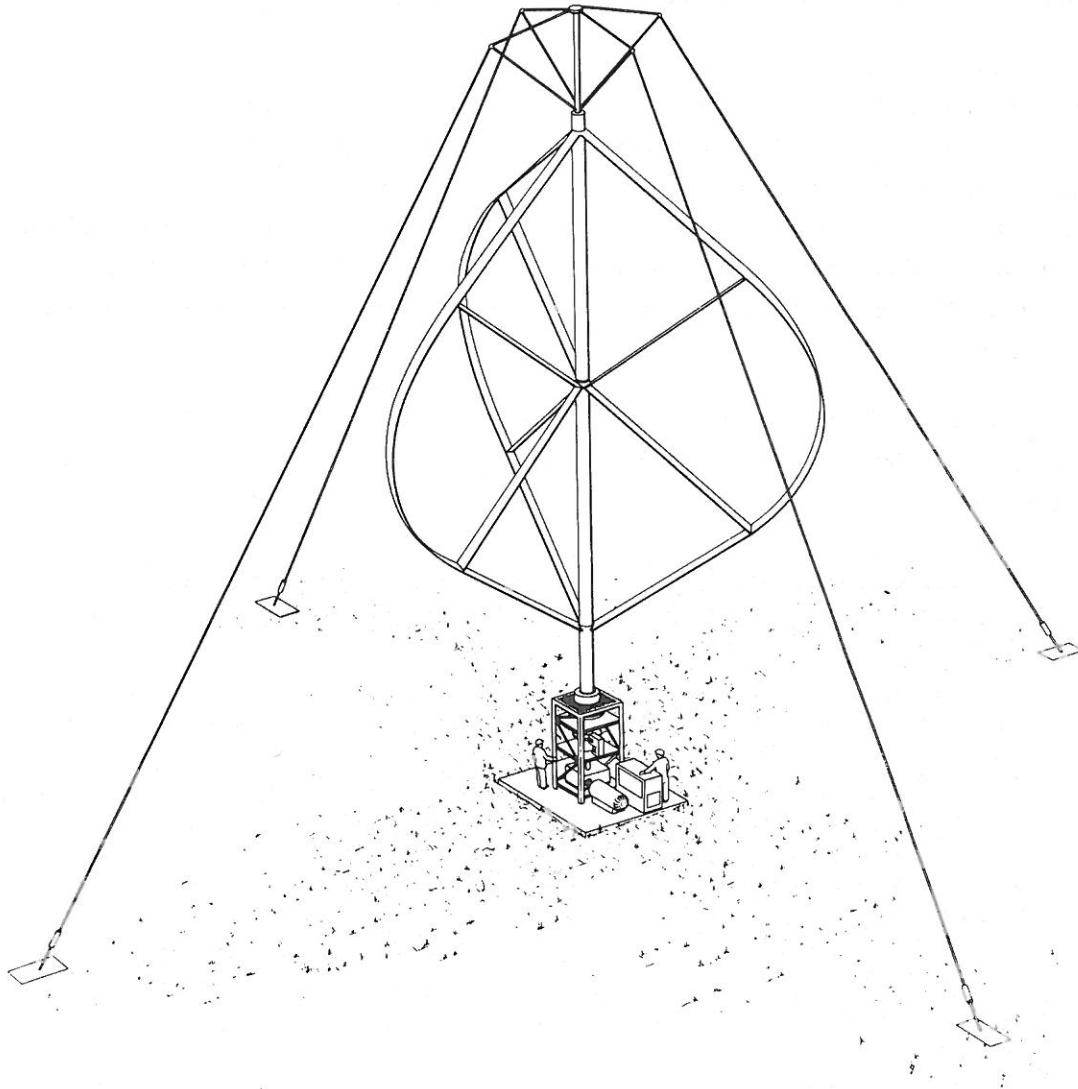
The basic concept of the Darrieus vertical-axis turbine (VAWT)¹ consists of fixed-pitch blades attached to a central, torque-transmitting shaft, as shown in the Frontispiece. Preliminary investigations of this device²⁻⁴ have noted a number of potential advantages over more conventional horizontal-axis systems. These advantages provided the motivation for establishing a program at Sandia to investigate further the feasibility of this turbine, particularly when used as an augmenting device to pump energy into an existing synchronous electrical network.

Based on the strategy that feasibility can best be established through a balanced program of hardware and analytical development, a twofold interactive technical approach has been adopted. This approach involves (1) development of the necessary analyses and empirical experience to design large, megawatt-range turbine systems that are economically optimized and (2) the use of this technical background, as it is developing, in conjunction with the experience and manufacturing facilities of private industry to design and construct a series of large VAWT power-generating systems. This series is to begin with a 17-m-diameter turbine connected to a 60-kW synchronous generator.

The quarterly report for the period January-March 1976 includes progress on the following briefly summarized technical program activities. Additional information on prior work can be found in Reference 7.

- A blade design and manufacturing contract was awarded to Kaman Aerospace Corporation, Bloomfield, CT. Kaman began work on the blade design on February 2, 1976. Blade delivery to Sandia-Albuquerque is scheduled for mid-October 1976.
- Structural analysis has been improved as a result of the ability to calculate coupled in-plane and out-of-plane motion of curved wind turbine blades with struts.
- A measurement technique to determine turbine performance was developed and successfully applied to the 5-m test turbine. Data for four turbine rotational speeds in the two-bladed configuration have been obtained with this method.
- Economic studies indicate a trend toward lower solidities and point up the importance of reduced transmission costs for optimized systems of ~1000-kW rated power.
- Wind tunnel tests of four symmetrical airfoil sections in the Reynolds number range of $0.35 - 0.7 \times 10^6$ and angles of attack up to 180° were completed at Wichita State University.

For discussion of specific aspects of this program, this report is divided into two major sections. The first, entitled "General Application Efforts," deals with the aerodynamic, structural, systems, and testing programs intended to be of general use for designers of vertical-axis turbine power systems. The second, "Specific Application Efforts," discusses details of design and testing currently being carried out on the proposed 17-m and the existing 5-m turbines.



Frontispiece - Artist's Concept of the 17-m Turbine

PART I
GENERAL APPLICATIONS EFFORTS

Aerodynamic Studies

Development work has continued on the multiple streamtube computer code. This code, which is capable of computing turbine power and blade aerodynamic loads for various turbine configurations, is being used for parametric studies and design of the 17-m system. Code modifications accomplished this quarter include utilization of the local blade Reynolds number to determine the appropriate aerodynamic forces acting on each blade element. For the synchronous grid application where the rotational speed remains constant, the local blade Reynolds number can easily vary by a factor of 8 over the windspeed range of operation. The maximum aerodynamic loads are extremely sensitive to the local Reynolds number variation; the power output is somewhat less sensitive, but still important.

The multiple streamtube code with variable Reynolds numbers was used to predict selected wind tunnel performance results. Figures 1 and 2 show a comparison of the theoretical calculations with experimental data for solidities of 0.3 and 0.13, respectively. The aerodynamic section data used in the calculations were taken from Strickland.⁵ The agreement between theory and data is quite good for the left-hand side of the power coefficient curve. For the relatively low tip-speed ratio range, the blades are "lightly loaded" and the theory has the most validity. The poor agreement between theory and data on the right-hand side of the power coefficient curve can be attributed to the fact that the model assumes that the downwind portion of the rotor sees the same induced velocity field as the upwind portion of the rotor. These calculations will be repeated with the section data from the Wichita State University tests (see Test Program section) as soon as these data are available.

Future computer code development activity will be centered around extending the multiple streamtube model to include the effect of struts and the effect that the upwind blade has on the downwind blade.

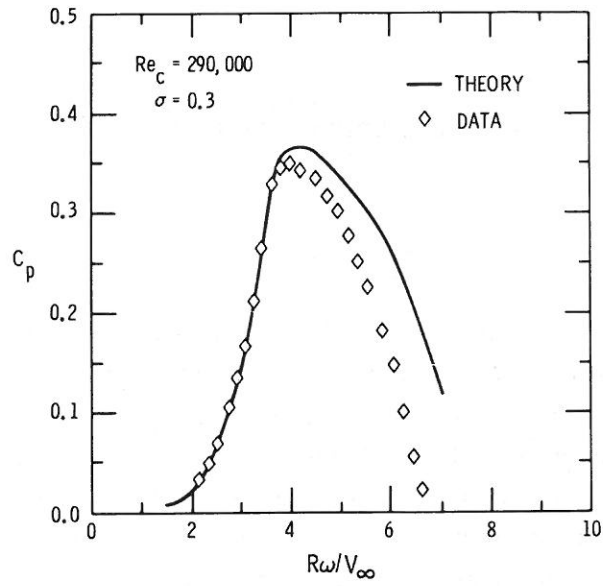


Figure 1. Comparison of Theory With Experimental Data, 0.3 Solidity

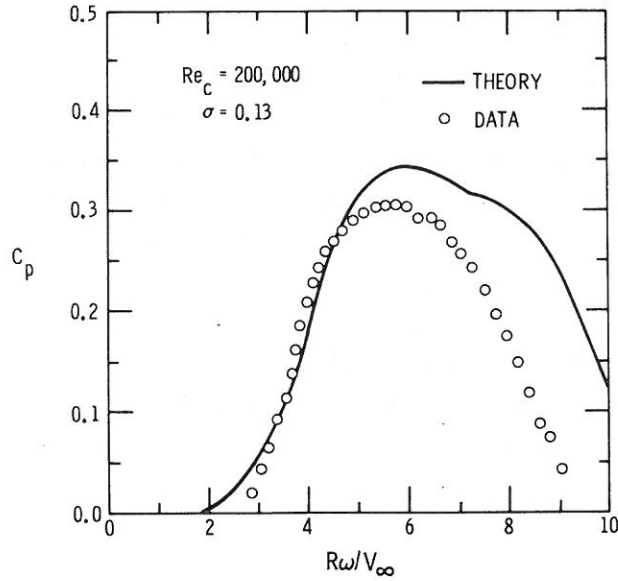


Figure 2. Comparison of Theory With Experimental Data, 0.13 Solidity

Structural Analysis

Significant progress has been made in four structural areas during this quarter: an analysis coupling out-of-plane (chordwise bending and twisting) deformations to in-plane (flatwise) deformations, calculations of system (tower/blades) natural frequencies, tower analysis, and effect of imbalance. The effect of imbalance is covered in the 17-m turbine section of Part II, Specific Applications Efforts.

Blade Analyses

The primary workhorse in the structural analyses of the blades has been a general-purpose, finite-element code. Two different beam elements have been selected from the element library to carry out blade structural analyses. The first, a curved-beam element with 4 degrees of freedom (2 displacements and 2 rotations) at each node, was used for analyses where motion in only the plane of the blade is allowed.* The application of this element was discussed in the previous technical quarterly report.⁷ During the quarter reported here, a straight-beam element with 6 degrees of freedom (3 displacements and 3 rotations) at each node was used to account for combined in-plane and out-of-plane deformations. The large-displacement capability of the code, which incorporates the effects of geometric nonlinearities, was utilized to model accurately the centrifugal stiffening in the blades. The finite-element model consisted of combinations of centrifugal forces, gravitational forces, and loading of the aerodynamic forces parallel and perpendicular to the blade chord. Application of the finite-element model to the 17-m turbine is addressed later in this report.

System Natural Frequencies and Mode Shapes

Frequency and mode shape analyses have been undertaken on a complete wind turbine assembly. The configuration used consisted of three blades, four guy cables, a cylindrical tower with outriggers for the cables, and a base (Figure 3). The computer program selected was the SAP4 finite-element code,[†] which was modified to include initial tension due to the centrifugal inertia of the blades. The initial tension was found by using the results of the computer program mentioned in the previous section, Blade Analyses. Results applicable to the 17-m turbine are presented in the section of this report entitled Special Applications Efforts.

The structural modes, which contribute significantly to the response, depend upon both the loading and the structure. A technique now being developed rank-orders the free vibration modes for a particular excitation.

* For the purpose of this report, in-plane motion is defined as motion in the plane formed by the tower axis and the locus of the centers of gravity of the blade cross section. Motion in the direction normal to the previously defined plane is termed out-of-plane motion.

† SAP4 is a structural analysis program for static and dynamic response of linear systems.

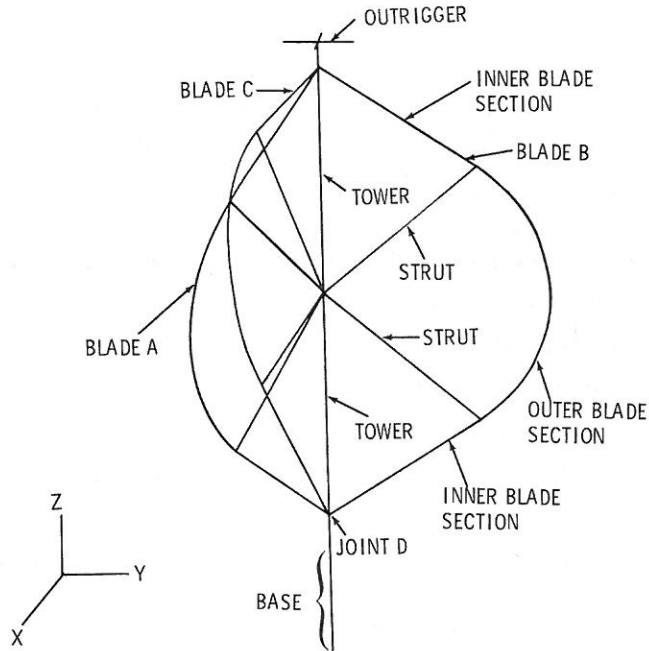


Figure 3. Finite Element Model of VAWT With Three Blades, Struts, and Four-Cable Outriggers

The rank-ordering procedure will be based on a measure of the overall system response attributable to a single mode. The process is repeated for each of the modes considered. The loading of the turbine will be considered attributable to a steady wind and, because of the constant turbine rotational speed, will result in an overall periodic excitation. The Fourier coefficients of the excitation are then to be computed by use of the fast Fourier transform. The steady-state response of the normal mode to each harmonic will be computed; the measure of the overall system response due to a single mode will be computed for each harmonic and summed over all harmonics. These norms can then be rank ordered to indicate the more dominant modes.

Tower Analysis

To provide technical support for determining the types of tower most suitable for vertical-axis wind turbines, analyses that permit a comparison of polygonal, prismatic trusses and tubular (cylindrical) shell-type towers have been developed.* The analysis consists, in part, of derivations of expressions that relate tower stiffness properties to tower geometry and material parameters. In the case of the truss-type tower, the necessary parameters are (1) bay length (a bay is that portion of the tower which is repeated lengthwise), (2) cross-bracing configuration, (3) the number of sides in the polygonal cross section, (4) element diameter (and, if hollow, wall thickness), (5) truss radius (radius of circumscribing circle), (6) truss length, and (7) the extensional and shear moduli. The

*To date only constant section towers have been considered.

tubular, shell-type tower is characterized by (1) overall diameter, (2) wall thickness, (3) tube length, and (4) the extensional and shear moduli. Clearly, the truss towers offer a greater design challenge than the tubular towers because of the larger number of parameters involved and the necessity to characterize the dependent interaction of the truss elements. The latter can be exemplified by the torsion problem where it is found that, because of element interaction, torsional resistance in each bay is developed by twisting, bending, shear, and extensional deformation in the truss elements. Stiffness properties used in the comparison exercises between trusses and shells are the axial, torsional, and bending components. Results indicate that, for specified torsional and bending stiffness values, a truss-type tower will yield the lightest weight structure, whereas, for a specified axial stiffness value, a tubular-type tower will be the most weight effective.

An example of this type of comparison is provided in Figure 4, where the ratio of the weight of the tubular tower to the weight of the truss tower versus the average bending stiffness is shown. Results are provided for three different truss element diameters, three different bay lengths, and a specified inside-to-outside tubular tower diameter ratio. These results suggest that, except for very long and slender bay geometries, truss towers can be made lighter than tubular towers having the same bending stiffness. It is also seen that increasing the truss element diameter generally reduces the weight effectiveness of the truss in the bending mode. Figure 5 shows a relationship between the geometries of truss of tubular towers that have equivalent bending stiffness. Results are given for three truss element diameters and are independent of bay length. Here, it is seen that truss radius increases rapidly with tubular tower diameter. Therefore, even though the truss tower is generally more weight effective than the tubular tower, it takes up considerably more space.

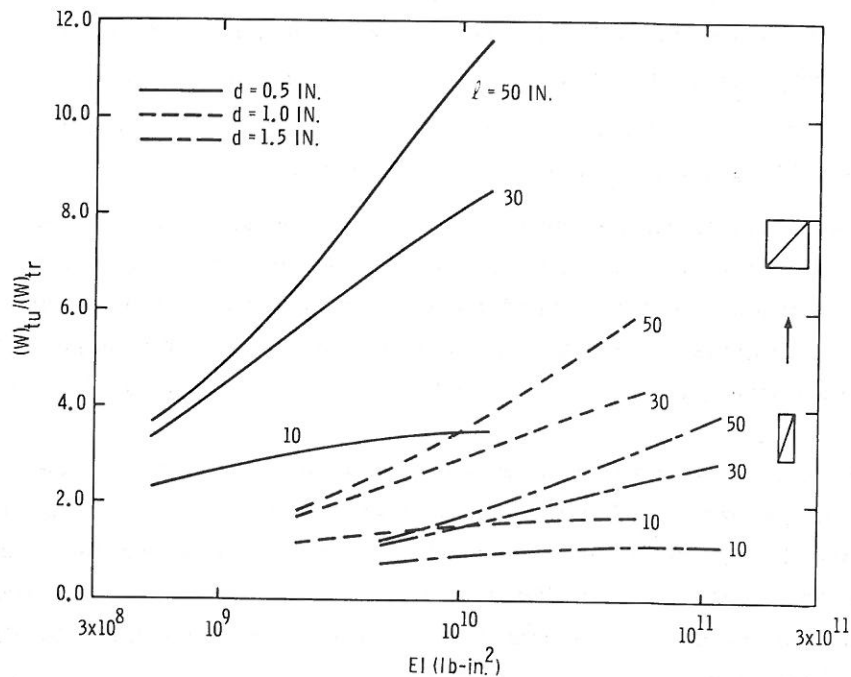


Figure 4. Ratio of the Weight of Tubular and Truss Towers That Have Equivalent Bending Stiffnesses

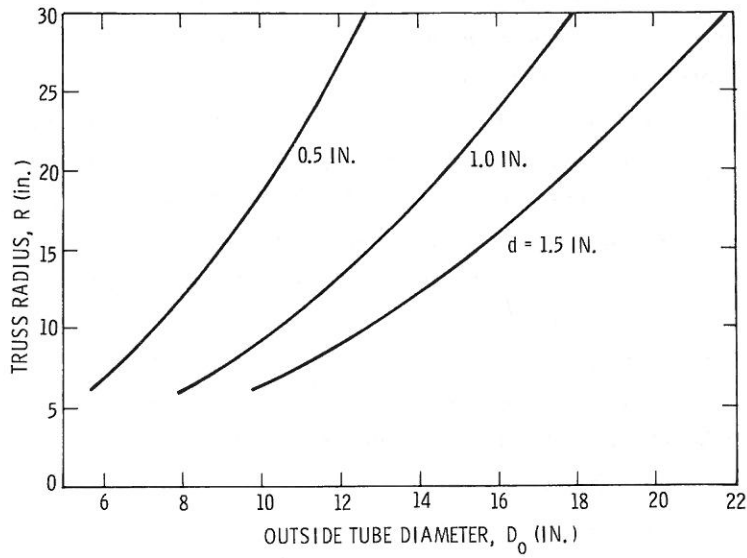


Figure 5. Relationship Between Geometries of Tubular and Truss Towers That Have Equivalent Bending Stiffnesses

Systems Studies

The objectives of economic studies emphasized this quarter are twofold:

- To identify tradeoffs and trends among system design parameters which lead to the definition of larger systems.
- To identify the cost of optimum systems in order to determine the role of the vertical-axis wind turbine relative to conventional alternatives.

To meet the above objectives, we visualize an iterative process, wherein the economics of VAWT systems are continuously updated as new performance and cost data become available. This section summarizes economic studies performed to date, with emphasis on trends related to system design; for example, in the areas of aerodynamics and structures. The effects of potential component cost savings are also indicated.

The economics of wind power generation systems involves a complex interplay of both cost and performance parameters. For example, aerodynamic studies indicate that such parameters as solidity, height-to-diameter ratio, and turbine configuration can produce a wide variety of performance characteristics. The effects of various features of the power coefficient on simple economic indicators have been investigated in an attempt to develop intuition for defining an economically attractive system.

Early analyses have indicated that blade cost and transmission cost are the two major contributors to total system cost. Blade cost can, to some degree, be related to the swept area of the turbine. Transmission cost is related to the rated output torque of the turbine. Thus, it would appear reasonable to use the terms E/A and E/T_R as measures of energy cost, where E is the annual energy output, A is the turbine swept area, and T_R is the rated torque. Inasmuch as these "economic indicators" are relatively easy to evaluate, a wide range of postulated systems can be investigated.

The particular functional form selected for the turbine power coefficient is depicted in Figure 6. Features of interest are the maximum power coefficient, $C_{P_{\max}}$; the tip-speed ratio corresponding to the maximum efficiency, λ_M ; the tip-speed ratio at zero efficiency, λ_R ; the tip-speed ratio at which power reaches a maximum with respect to windspeed, λ_K ; and an exponent that defines the turbine power output for high windspeeds, $N \geq 3$.

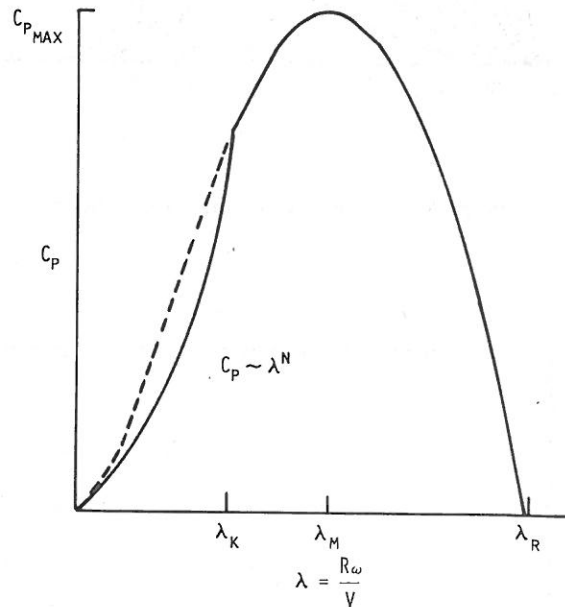


Figure 6. Model Power Coefficient

Figures 7 and 8 show a typical result from computations of E/A and E/T_R as functions of $R\omega/\lambda_M$ and λ_K/λ_M . The following observations can be made:

1. E/A and E/T_R increase with $C_{P_{\max}}$; higher efficiency means more energy extracted from the wind.
2. E/T_R increases with λ_M ; rated torque for a given rated power can be decreased by increasing λ_M , which is a measure of turbine rotational speed.

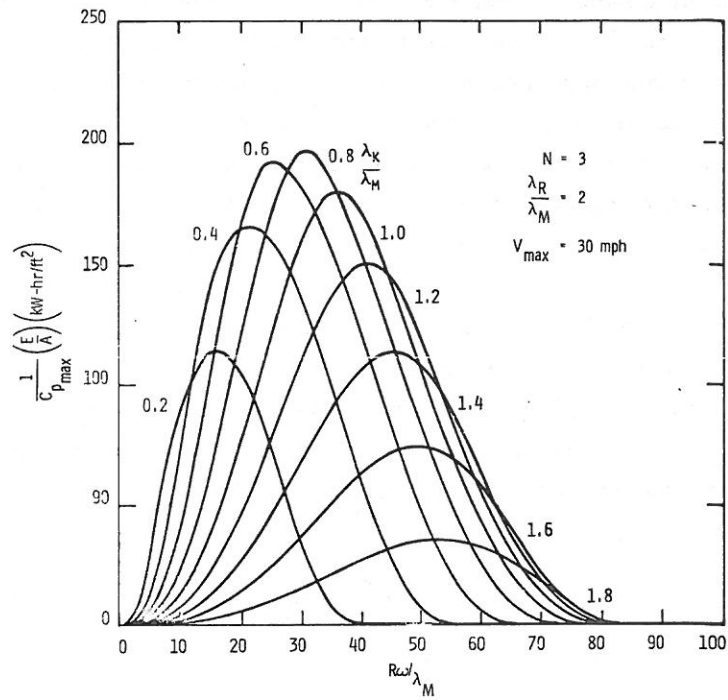


Figure 7. Energy Per Unit Swept Area

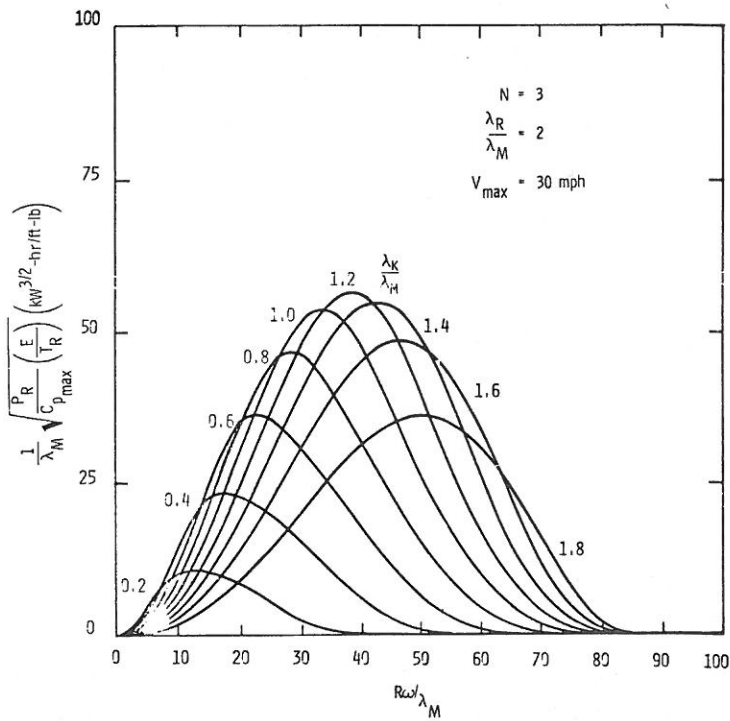


Figure 8. Energy Per Unit Rated Torque

3. E/A and E/T_R reach maxima with respect to $R\omega/\lambda_M$. If ω is small, power is small, implying little energy; if ω is large, power is large but corresponding windspeeds are rare, implying little energy.
4. E/A and E/T_R , when maximized with respect to $R\omega/\lambda_M$, also achieve maxima with respect to λ_K/λ_M . If λ_K/λ_M is small, component efficiency at reduced loads becomes small; if λ_K/λ_M is large, turbine efficiency is reduced.
5. Although not demonstrated in Figures 7 and 8, the exponent N should be close to 3 in order to achieve a constant power/windspeed relationship. Finally, λ_R/λ_M should be large so that the turbine efficiency characteristic is broadened.

An economic model that accounts for the actual costs of the turbine, transmission, and generator indicates that a value of λ_K/λ_M intermediate to the values of Figures 7 and 8 should be chosen. It should be noted that this value will depend on the relative component costs, but is around 1.

The foregoing discussion has indicated that several features of the power coefficient can substantially influence the economics of wind power systems. Results from aerodynamic studies suggest, however, that these features do not vary independently. For example, Figure 9 shows power coefficients for several values of turbine solidity calculated with the single-streamtube aerodynamic performance model. Although λ_M is increasing, as desired, with decreasing solidity, $C_{p_{max}}$ is decreasing. Coupling of the features is similarly obtained from variations of the other aerodynamic design parameters.

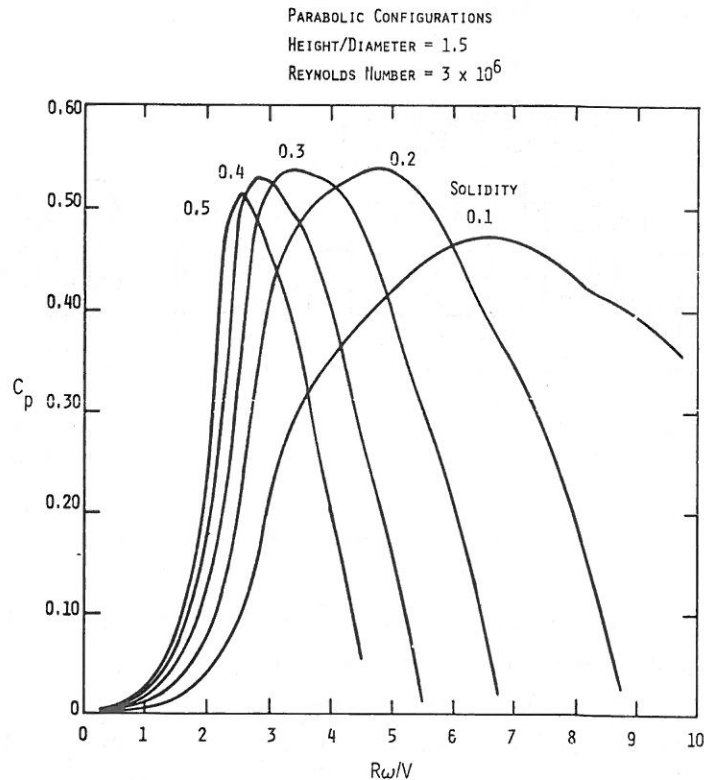


Figure 9. Power Coefficients From Aerodynamic Model

Figure 10 is a flow chart of the economics model, which has been structured to accept updated cost and performance data as they become available. Power coefficient as a function of tip-speed ratio, turbine solidity, and Reynolds number is based on extrapolations of both wind tunnel test data and aerodynamic performance model predictions. Also included in the model are component efficiencies and costs. In particular, the turbine cost has been made to depend on solidity, σ ; number of blades, N ; and radius, R , in accordance with

$$\frac{\sigma^{1.2} R^{2.2}}{N^{0.2}}$$

If resonances and centrifugal loads only are considered, the blade wall thickness need not grow with scale-up, and cost is proportional to R^2 . Aerodynamic loads, however, appear to require some increase of thickness. For the examples that follow, cost has arbitrarily been made proportional to $R^{2.2}$.

A reference case formulated to illustrate results of the economic analysis includes the following:

1. Turbine cost is increased to reflect use of struts that have the same cross section as the blades.
2. Blade cost, based on roll-formed steel construction is \$10/lb.
3. Site median windspeed is 12 mph.

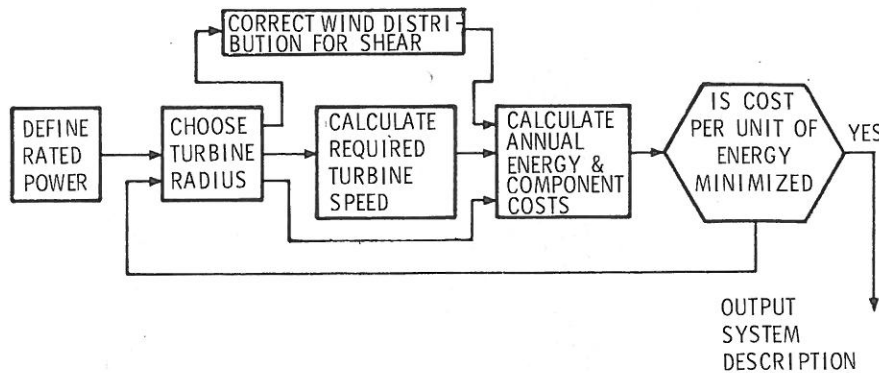


Figure 10. Flow Chart of Economics Model

Figure 11 shows energy cost for optimum systems with rated power up to 1000 kW. Turbine diameter and rotational speed are noted for the 500- and 1000-kW systems. For rated power below ~200 kW, energy cost is rising rapidly; such systems would not appear to be cost effective. For rated power above 200 kW, energy cost is judged relatively constant within the accuracy of the model. The selection of solidity equal to 0.1 and number of blades equal to 3 is discussed in the following paragraphs.

Low solidities are attractive because of decreased blade cost and increased tip-speed ratios. As solidity is decreased, however, the maximum power coefficient is reduced. Figure 12 shows the variation of energy cost with solidity when the number of blades is fixed at three. As anticipated, an intermediate value of solidity results in the lowest energy cost as a result of the reduction in $C_{p_{max}}$ with decreasing solidity.

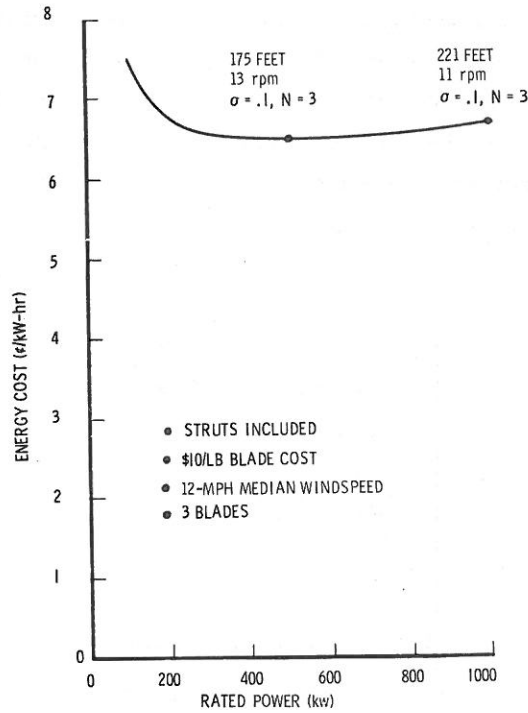


Figure 11. Reference Cost Case

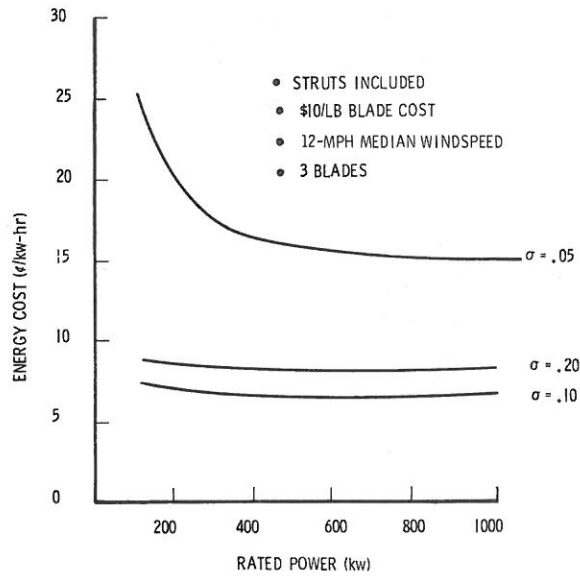


Figure 12. Variation of Energy Cost With Solidity

A given solidity can be achieved by varying the number of blades and chord/radius ratio. As depicted in Figure 13, solidity is linearly dependent upon chord/radius for a fixed number of blades. When the number of blades is increased, the required value of chord/radius is reduced, thereby tending to reduce the Reynolds number. This last point is important, since it appears from wind tunnel test data that λ_K/λ_M is decreasing as Reynolds number is increasing, thereby reducing energy output. To determine how small chord/radius can get, structural requirements must be considered. Alternatively, the limits on chord/radius ratio can be used to determine the required number of blades. This is illustrated in Figure 14, which shows the variation of energy cost with chord/radius and the number of blades. If, for example, the minimum allowable chord/radius ratio is 0.06, two blades would be chosen. However, three blades would give a lower energy cost at a chord/radius of 0.03.

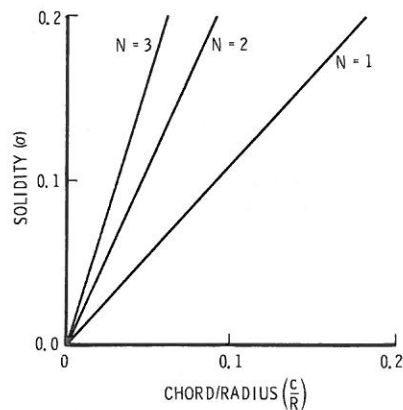


Figure 13. Variation of Solidity With Chord/Radius

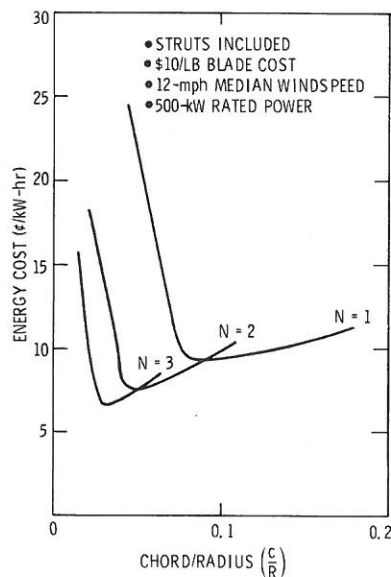


Figure 14. Variation of Energy Cost With Chord/Radius

Three areas for potential cost reduction are the blades, the struts, and the transmission. Figure 15 shows the individual effect, relative to the reference case, of (1) reducing the blade cost to \$5/lb, (2) halving the transmission cost, and (3) eliminating the struts. It can be seen that each cost reduction has a substantial effect on energy cost. Figures 16 and 17 show the combined effects of these cost reductions on energy cost for site median windspeeds of 12 and 18 mph, respectively.

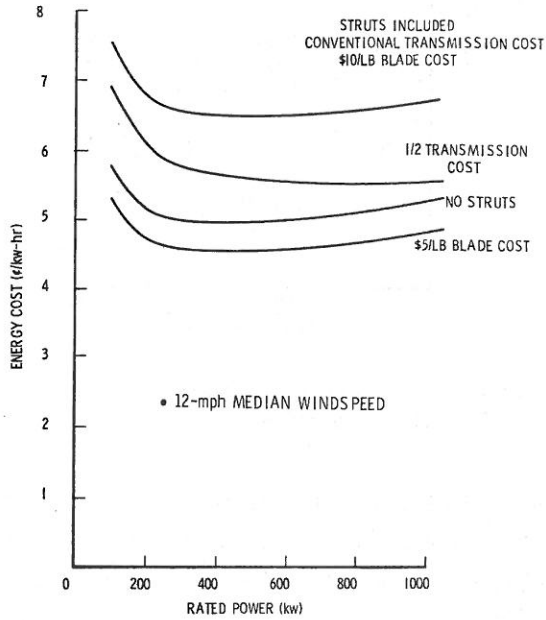


Figure 15. Effects of Component Cost Reductions

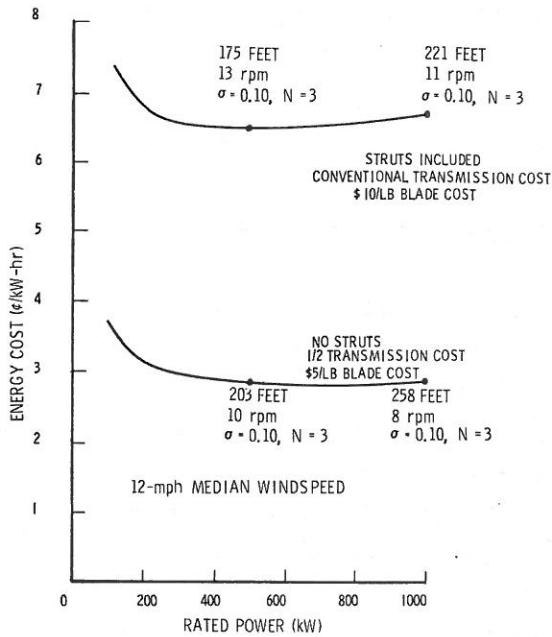


Figure 16. Combined Effects of Potential Cost Reductions

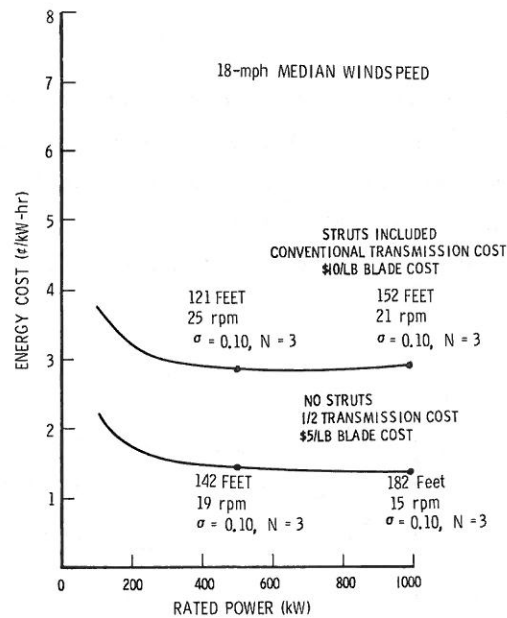


Figure 17. Combined Effects of Potential Cost Reductions

Further effort is needed with regard to definition of aerodynamic performance, structural requirements, and component costs. Currently, aerodynamic performance is based on extrapolations of wind tunnel data over an order of magnitude in Reynolds number, and trends of analytic predictions are consistent with these extrapolations. Structural requirements must be defined for larger systems. Finally, costs of such components as the turbine, tower, and transmission must be defined in more detail. It is anticipated that design, fabrication, and testing of the 17-m turbine system will provide much of the needed information.

Test Program

Test Facility Automatic Control and Data Acquisition

The goal of this effort is to minimize the manpower costs of operation and data reduction by using cost effective automation capable of operating and monitoring the complete wind turbine system independent of on-site personnel. To achieve this goal, the Sandia Laboratories Wind Turbine Test Facility is equipped with a microprocessor system and a number of peripheral electronic devices that interface the processor with the turbine's power system, operating sensors, anemometers, and output recording devices. The microprocessor system is based on an Intel Intellec-80 with an ICOM floppy disc magnetic storage system.

Figure 18 is a simplified block diagram of the microprocessor system for automatic control of the VAWT. In essence the microprocessor is an intelligent automatic operator which runs the start motor, generator, and/or brakes as a function of the wind conditions and the state of the VAWT.

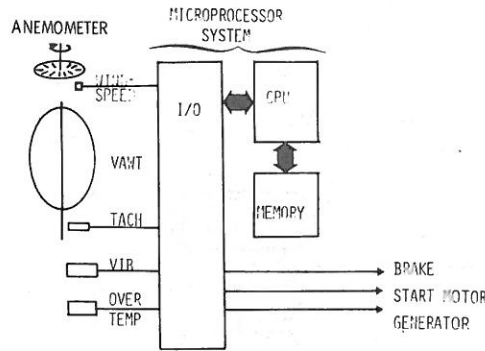


Figure 18. Automatic Control of VAWT

Based on windspeed history, a determination (Figure 19) as to when to run the VAWT is made by the microprocessor program. If adequate windspeed is observed for a sufficient time, the turbine is started. If the windspeed falls below an acceptable level for more than a prescribed time, the turbine is shut down. Both the windspeed and time criteria for running are programmable, and selections of values may depend on the site and particular turbine characteristics. Once the turbine is running, the microprocessor monitors such sensors as bearing and generator temperatures, structural vibration, turbine shaft speed, and electrical power. If an unusual condition is observed, the system will notify responsible personnel. If a malfunction occurs, the system will execute an orderly shutdown. A microprocessor wind turbine controller that displays the above functions has been demonstrated at the Vertical-Axis Wind Turbine Workshop in May 1976.

Figure 20 displays block diagrams of wind instrumentation systems based on the conventional manual method and an automated data acquisition approach. In the manual approach the anemometer and wind turbine torque data are stored on a strip chart record. The strip chart is then digitized, and the data are stored on magnetic tape for input to a computer for data processing and output plotting. This approach has a number of severe drawbacks. First, the strip chart recording is not appropriate for taking accurate data over extended periods of time. The amount of chart paper required for long runs is enormous, and the accuracy obtained is inversely related to the paper's speed because of ink smear and noise. Once the long lengths of recordings are made, the information must be digitized for computer processing. This procedure requires extensive, time-consuming manual labor.

The automated approach alleviates the above problems by performing the analog-to-digital (A/D) conversion directly from the test instruments. The digital data are processed by a microprocessor and recorded onto a paper tape or magnetic cassette or fed directly to a large computer via a phone link. A further step may be taken by using digital instruments to eliminate the A/D converter entirely.

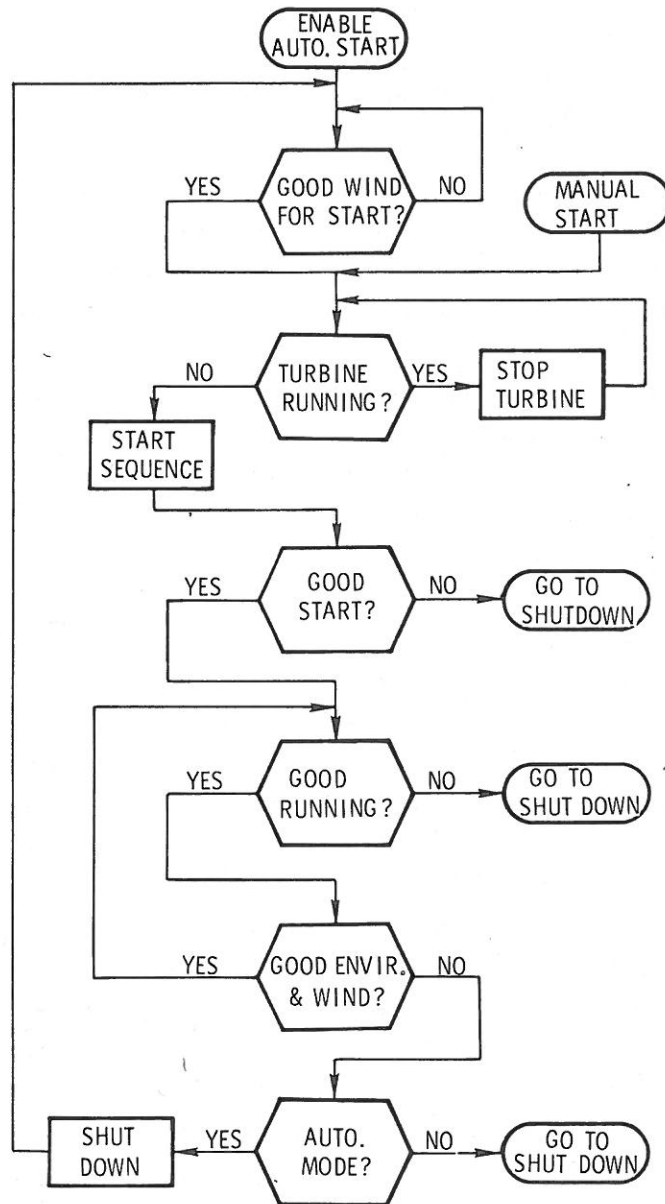


Figure 19. Microprocessor Program Flow Chart for VAWT

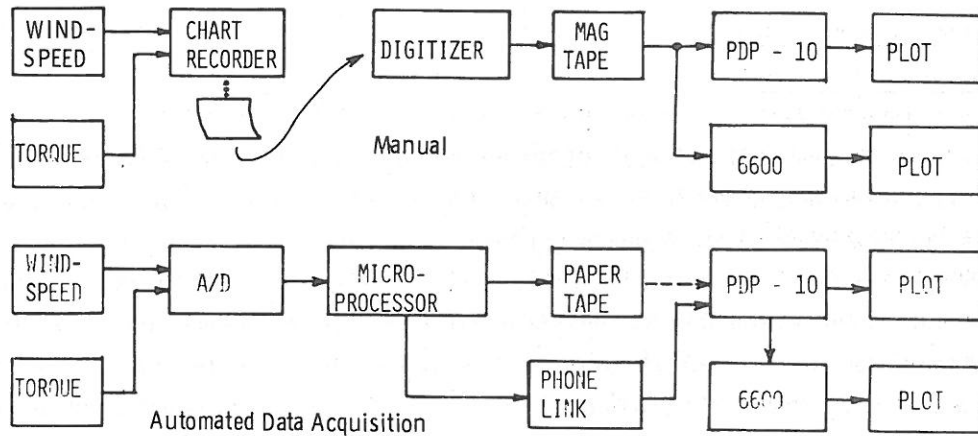


Figure 20. Wind Instrumentation Systems

Wind Tunnel Performance Tests

The wind tunnel performance test results reported in the previous quarterly continue to be analyzed. Figure 21 compares performance data for two of the Sandia configurations tested at constant freestream velocity with NRC data presented by South and Rangl.⁶ The NRC test conditions were 50- to 250-rpm turbine speed and 3.05- to 6.1-m/s (10- to 20-ft/s) tunnel speed. The NRC data exhibit a slightly higher $C_{p,max}$ occurring at a higher tip-speed ratio and a lower tip-speed ratio for the runaway condition. There are obvious discrepancies between the two data sets; the cause for the disagreement will be explored in greater detail in the upcoming quarter.

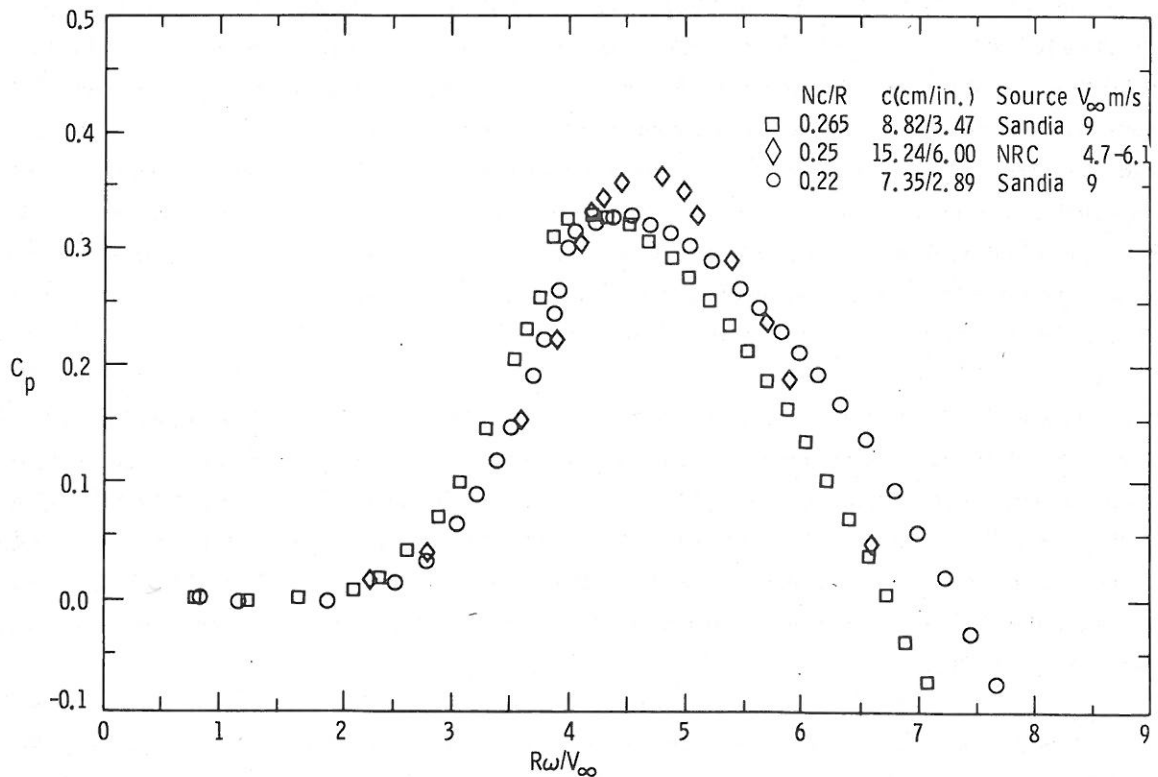


Figure 21. Comparison Between Sandia and NRC Experimental Performance Data

Wind Tunnel Section Tests

Sandia Laboratories contracted with Wichita State University to construct four different symmetrical airfoil sections and to test the models at angles of attack to 180° for three differing Reynolds numbers. One of the Reynolds numbers was to be as low as could be obtained and still be within the operational range of their facility and balance system. The purpose of these tests was to obtain needed section data for the NACA-0012 airfoil over the angle-of-attack range of interest at as low a Reynolds number as possible. In addition, similar section data for a thinner (NACA-0009) and a thicker (NACA-0015) airfoil were deemed necessary to aid in determining the optimum airfoil for future turbines. Also, a nonstandard airfoil, a modified-0012 designated NACA-0012H, was tested.

The four symmetrical airfoil models were constructed of aluminum to standard wind tunnel model tolerances by Wichita State University. All models had a 15.24-cm (6-inch) chord with a 0.91-m (3-foot) span. These models were of standard airfoil cross section: NACA-009, -0012, and -0015. The fourth airfoil, which was nonstandard, was a modification of the NACA-0012 provided by Raymond M. Hicks of NASA/Ames Research Center. The modification was designed with the aid of a computer program to increase the maximum lift coefficient of a given airfoil by reducing the leading edge pressure spike associated with subsonic airfoils. The resultant airfoil designated NACA-0012H remained at 12 percent thick.

The airfoils were tested in the Walter H. Beech Memorial Wind Tunnel at Wichita State University. The wind tunnel has a 7- x 10-foot (2.13- x 3.05-m) cross section fitted with floor-to-ceiling two-dimensional inserts for testing two-dimensional airfoil sections. These inserts in the center of the test section act as flow splitters to form a separate test section 3 feet (0.92 m) wide by 7 feet (2.13 m) tall. Part of the total airflow in the wind tunnel goes through the 3- x 7-foot section and part flows by each side. The 3- x 7-foot section is separately instrumented with pitot/static probes for the determination of flow conditions within that section. A wake survey probe was installed in the wind tunnel for a separate series of tests to obtain the airfoil section drag at low angles of attack for all airfoil models.

The airfoil models were attached to the end plates in the walls of the two-dimensional inserts. These end plates are the attachments to the angle-of-attack control mechanism and the facility balance system. The models were tested at three Reynolds numbers, nominally 0.35×10^6 , 0.50×10^6 and 0.70×10^6 , through angles of attack to 180° . The angle of attack control mechanism has an approximate range of 60° , which requires that the model be reoriented on the end plates 3 times to complete the full range of angles of attack to 180° . This allowed for some overlap of data near 40° , 90° , and 130° .

Data for each airfoil were first obtained over the range of -24° to $+32^{\circ}$ (increasing α) and then from $+32^{\circ}$ to -24° (decreasing α) for the three Reynolds numbers. This was done to obtain the hysteresis loop in the region of airfoil stall. All full-range data were obtained with increasing

angles of attack to 180° . Lift, drag, and moment data were obtained from the balance system. All the data were corrected for wake and solid blockage, buoyancy, upwash, and turbulence factor. The turbulence factors used to correct the Reynolds numbers to 0.35×10^6 , 0.50×10^6 , and 0.70×10^6 were 1.38, 1.29, and 1.13, respectively. All the tests reported here were performed on aerodynamically smooth airfoils.

Figure 22 is a composite showing the lift data for the four airfoils at a Reynolds number of 0.7×10^6 . Data shown are for increasing angle of attack for positive angles and decreasing angle of attack for negative angles. This demonstrates the increased performance of the NACA-0012H and the favorable performance of the NACA-0015.

The data for the drag coefficients were obtained by the balance system and corrected by data obtained in the angle-of-attack range of positive to negative stall by a wake survey method. This corrected the force data for drag on the end plates. At present, the drag data between positive and negative stall seem low. These low values of minimum drag for the airfoils are of concern and will require careful scrutiny. The presence of hysteresis in the coefficient of lift data obtained by quasi-steady-state methods suggests the advisability of including it in computer solutions of vertical-axis wind turbine performance. This hysteresis is much more pronounced with the thicker airfoils; i. e., the NACA-0012H and NACA-0015. The data obtained are the start of a data base that will be extremely useful in the analysis of vertical-axis wind turbines. It is intended to extend the data base by additional tests of a NACA-0012 airfoil with a 15-inch (38.1-cm) chord at Reynolds numbers of 0.70×10^6 to 2×10^6 so that section data are available in the operating Reynolds number range for the Sandia Laboratories 17-m system.

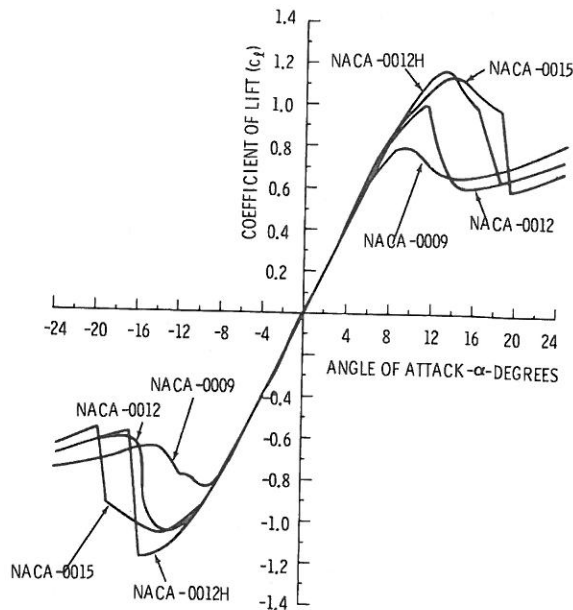


Figure 22. Lift Coefficients for Four Airfoil Sections at Reynolds No. $\approx 0.7 \times 10^6$

PART II
SPECIFIC APPLICATIONS EFFORTS

The 17-m Turbine

Introduction

The design and construction of the 17-m vertical-axis wind turbine, which will be the largest of its type in the U. S. , is one of the primary FY 76 goals of the Sandia Vertical-Axis Wind Turbine Program. The main purpose of this device will be to serve as a research tool that is large enough to approach the economically optimum sizes suggested by our systems studies. It is only through the exercise of design, construction, and operation of such a turbine that an accurate realization can be made of the advantages, disadvantages, and technical problems associated with vertical-axis power-generation systems.

It is believed that the design approach adopted for the 17-m turbine will yield an operational unit that will fulfill the fundamental objectives of the program. There is no illusion, however, that this turbine represents an optimum wind energy system. Indeed, the knowledge necessary to define optima depends on experience, and this is only beginning to be accumulated.

A blade request-for-quotation (RFQ) (see Appendix A of Reference 7) was sent to 58 manufacturers in early fall 1975. This RFQ specified mainly the geometrical and structural requirements of the blades and left the actual analysis, design, and construction of the blades open to the manufacturer. Kaman Aerospace Corp. of Bloomfield, CT, offered a design and analysis approach using helicopter technology, which was felt to have a high probability of success. A contract has been placed with Kaman for an expected blade delivery date of fall 1976. The Sandia-designed tower, tiedowns, and electrical equipment will be completed at that time so that the turbine can be assembled and erected immediately.

Although the RFQ approach to blade procurement was successful in that operational blades will be obtained within the program time scales, this approach is not without difficulties. For example, response to the RFQ was limited, apparently because private industry was uncertain as to how to analyze and design these unique blades. Also, the helicopter-type blade construction methods selected are expensive, the blade costs being of the order of \$50/lb, even for high-production units. To alleviate these problems, an in-house blade design program now being pursued will proceed in parallel with the Kaman effort but with longer time scales. The in-house design will emphasize low-cost construction methods and utilize the latest information on turbine loads, structural analysis, and aerodynamic requirements as generated by the overall wind power program.

This program, together with the experience accumulated by Kaman in its design and manufacturing program, should yield lower cost blades on subsequent turbines.

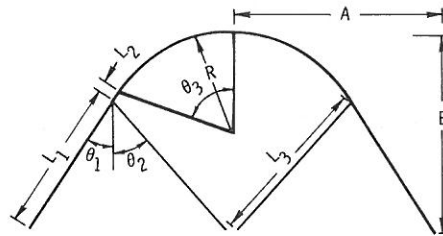
The following sections document technical achievements made during the reporting period in support of the 17-m turbine program.

Structural Analysis

Blade Analyses -- The analysis reported addresses the blade being designed and built by Kaman for the Sandia 17-m wind turbine. As shown in Figure 23, the blade consists of two straight sections and a center circular section. Struts are included between the blade and the shaft to provide additional support. The geometric properties used in the analysis are also given in Figure 23. The struts have the same cross section as the blade (Figure 24). The load-carrying portion of the blade is a 6061-T6 aluminum leading-edge D-section and trailing-edge spline. The material and elastic properties of this blade are tabulated in Table I.

TABLE I

EI_1 (flatwise flexural stiffness)	31.63×10^6 lb-in. ²
EI_2 (chordwise flexural stiffness)	1246×10^6 lb-in. ²
EA (longitudinal stiffness)	52.16×10^6 lb
W (linear density)	0.572 lb/in.
GJ (torsional stiffness)	25.06×10^6 lb-in./rad.



$R = 220.0$ in.	$L_3 = 272.07$ in.
$A = 325.47$ in.	$\theta_1 = 33.24^\circ$
$B = 315.24$ in.	$\theta_2 = 41.12^\circ$
$L_1 = 245.07$ in.	$\theta_3 = 56.76^\circ$
$L_2 = 13.0$ in.	

Figure 23. Wind Turbine Blade Geometry
(Distance from blade attachments to tower centerline is 14.0 in.)

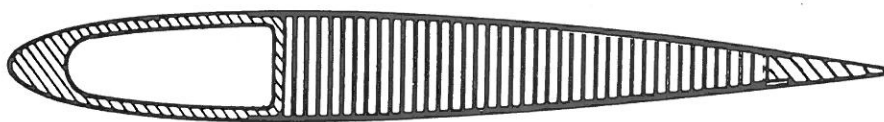


Figure 24. Kaman Blade Cross Section

To date, the blade structural analyses include the following loading conditions:

1. 0-rpm, 0-mph wind, gravity included
2. 0-rpm, 150-mph wind, gravity included
3. 52.5-rpm, 60-mph wind, gravity neglected (normal operating condition)
4. 75-rpm, 80-mph wind, gravity neglected (runaway condition)

The blade deflections for the first condition are shown in Figure 25. The ground is to the left in the figure, and deflections are magnified by a factor of 10. The maximum stresses, which are approximately 1700 psi, are well below yield.

The second loading conditions represents severe gust loading with the wind turbine in a parked mode. Figure 26 shows the deflection for an inward-directed 150-mph wind. The deflection shown is actual. Stresses induced in the blade and struts are high, the maximum being approximately 20 000 psi, but are less than yield. However, large compressive forces that exist in the straight sections may lead to a buckling problem. Studies currently being directed to this possible buckling condition may provide an upper limit for winds that the turbine can withstand.

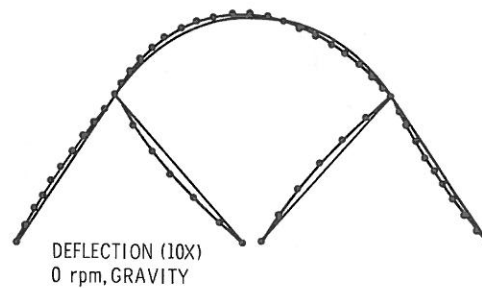


Figure 25. Nonrotating In-Plane Deformation

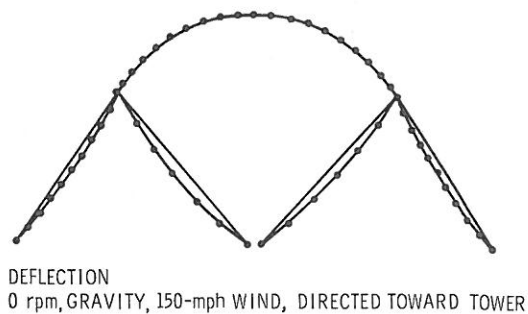
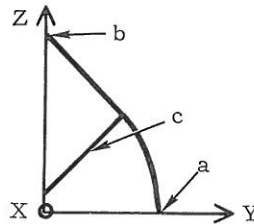


Figure 26. Nonrotating In-Plane Deformation
With Severe Gust

As outlined, the third and fourth loading conditions omit gravity. Without gravity the blade model can be simplified since, because of symmetry considerations, only half the blade need be modeled. An investigation was performed on a blade rotating at 75 rpm (a runaway condition), with and without gravity, to determine the effects of this omission. Results showed that there was less than a 10 percent difference in maximum stresses. This indicates that for relatively high rotational speeds gravity can be neglected.

Results presented here for the third and fourth loading conditions are restricted to the blade assembly with struts. One reason for this is that analyses of blade models without struts indicated that stresses in the spline of blade, caused by out-of-plane loads, were well above the yield point of 6061-T6 aluminum. The inclusion of the struts alleviates these high stresses as is shown in Table II.

TABLE II
Example Deformation and Stress Results



<u>Load Condition</u>	<u>X Displacement at Point a (in.)</u>	<u>Y Displacement at Point a (in.)</u>	<u>Z Angle of Twist at Point a (deg)</u>	<u>Maximum Stress (ksi)</u>	<u>Maximum Stress Location</u>
52.5 rpm, 60 mph					
C - A	5.29	0.60	-2.15	16.52	b
C + A	4.66	1.42	-1.84	16.56	b
C only	0.00	1.09	0.00	9.51	c
75 rpm, 80 mph					
C - A	9.16	1.14	-3.73	29.11	b
C + A	7.38	2.40	-2.85	28.05	b
C only	0.00	1.97	0.00	16.18	c

In each case, quasi-static analyses were completed for three different blade positions. The first, designated by (C-A), corresponds to the point in the cycle where the aerodynamic forces are maximal, with the radial component directed in the direction opposite from the centrifugal forces. The symbol (C + A) denotes the case where the aerodynamic forces are also maximal, but the radial component is in the direction of the centrifugal forces. The position designated by (C) corresponds to the case where aerodynamic forces are zero.

For the normal operating condition in Table II (52.5 rpm, 60 mph) the maximum out-of-plane displacement is 5.29 inches, with a corresponding angle of twist of -2.15° . Deformations of this magnitude are not thought to degrade turbine performance significantly; however, further attention is being devoted to this area. A maximum stress of 16.56 ksi occurs at the root of the blade in the splines. The stress at this point varies from this maximum down to a minimum stress of 1.04 ksi twice per cycle. By using these data, along with similar results for other operational speeds and winds, life-cycle estimates for a particular wind turbine site can be obtained.

For the runaway condition (75 rpm, 80 mph) performance degradation is not an issue, nor is fatigue since the number of cycles at this condition is assumed to be low. The main concern is that blades do not yield. The results shown in Table II show the maximum stress to be less than the yield value of 35 ksi for 6061-T6.

The results for these last two loading configurations are thought to be on the conservative side. For example, the aerodynamic loads used do not take into account Reynolds number effects that may reduce the loads by as much as a factor of 2. Also, the aerodynamic loads are actually dynamic, and the blades may not have time to respond fully to these time-varying forces.

The preliminary results reported here show that a software capability exists for analyzing the strutted and unstrutted blades for the Sandia vertical-axis wind turbine. They also show that the Kaman-designed blades are structurally adequate for the loading conditions addressed.

Effect of Imbalance -- An analysis to determine the effects of mass imbalance on the 17-m VAWT was completed. The initial concern was that the imbalance could cause shaft deflections and subsequent high bearing loads. In addition, there was concern that a condition might be created that would lead to an unstable self-excited motion.

A simple model, known as the Jeffcoat model in the literature, was made of the 17-m turbine. It consists of a centrally located unbalanced disc attached to a massless elastic shaft. Parameters for the model were obtained by computing the effective mass and stiffness for the turbine.

It has been determined that the present maximum operating speed is sufficiently below the resonant condition that only nominal deflections and bearing loads will be encountered. Also, it has been shown that the present operating speeds are well below the speed necessary to cause the onset of the unstable self-excited motion.

Tower/Blade System Natural Frequencies and Mode Shapes -- The natural frequencies of the system were determined by using the SAP4 computer program. The tower was assumed to be in the form of a circular tube, with a 20-inch O.D. and 19-inch I.D. The rotational speed used was 75 rpm. The lowest natural frequency occurs when the principal motion is movement of the blades out of their plane (Figure 27). Frequencies of approximately 2.75 Hz are predicted. Motion in the plane of the blades yields frequencies of approximately 3.6 Hz for the mode that is primarily strut motion and 5.0 Hz (Figure 28) for the mode that is primarily blade motion.

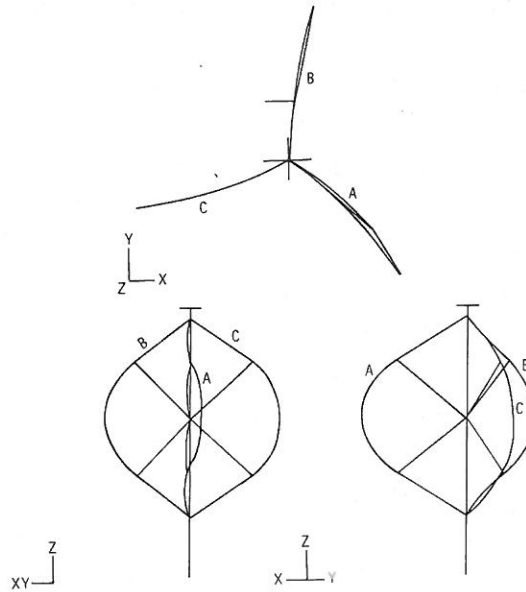


Figure 27. Isometric View of VAWT. Example of Out-of-Plane Blade Mode Shape

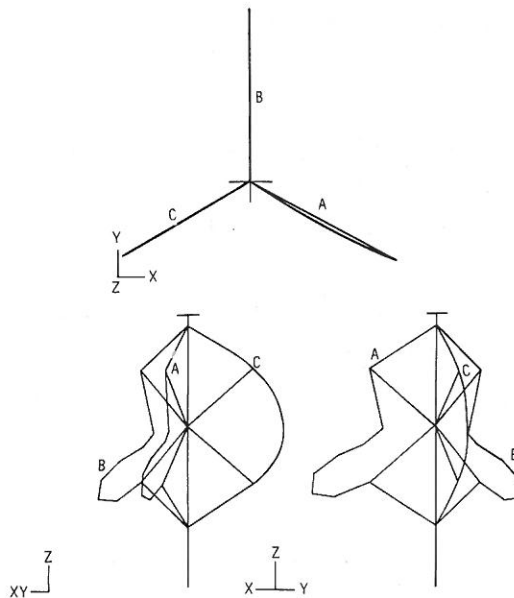


Figure 28. Isometric View of VAWT. Example of In-Plane Blade Mode Shape

The change in the results—either of pinning joint D (i. e., no moment carrying capacity) or of using the tower-bending stiffness—was determined (see Figure 3). A considerable reduction in the frequency (approximately 40 percent) for the deformation shape shown in Figure 29 was obtained.

Note that some of these natural frequencies are below the design goal of 4.5 Hz at a turbine rotational speed of 75 rpm (see Appendix A of Reference 7). The effects of these low frequencies are being studied in a modal participation analysis, described in Part I, General Applications Efforts.

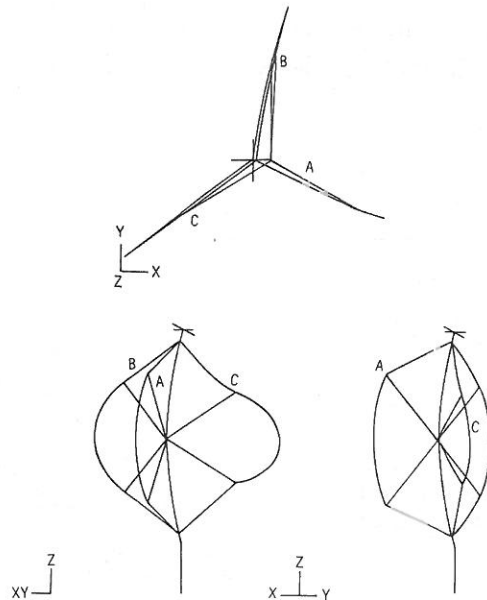


Figure 29. Isometric View of VAWT. Example of Tower Bending Influenced Mode Shape

Tower Design -- The tower for the 17-m turbine must be designed to withstand axial loads due to the tiedown, axial components of the blade root loads, and turbine weight. It must also withstand torsional loads due to blade root moments resulting from aerodynamic torques and turbine inertial loads, as well as flexural loads due to radial components of the blade root loads and aerodynamic drag. Finally, the resonant frequencies of the tower or those which involve the tower should be above 4.5 Hz, which is 3 times the turbine runaway speed of 75 rpm, plus 20 percent. All these conditions place requirements on the tower that can be characterized by axial, torsional, and flexural stiffnesses; buckling resistance; and load-carrying capabilities. Design curves for these requirements have been developed. These design curves cover wide ranges of parameter values, as illustrated in Figures 30 and 31. Figure 30 illustrates the ratio of the weight of a tubular tower to the weight of a truss tower (with the same torsional stiffness) versus the torsional stiffness. It appears that for any required torsional stiffness a lightweight, truss-type tower can always be designed. However, Figure 31 shows that a truss tower will have a larger diameter than a tubular tower with the same torsional stiffness. Since both size and weight are important considerations in wind turbine tower design, requirements for a tubular tower were examined further and

are presented in Figure 32. Here, the total weight of the tower is shown versus tower diameter for three ratios of inside to outside diameters. The intersecting curves labeled bending and torsion are connecting points on the weight curves that represent minimum design to meet the bending and torsional natural frequency requirements (must be ≥ 4.5 Hz). The cross-hatched curves then represent minimum design values for tubular towers that will meet the natural frequency requirement of 4.5 Hz. If the minimum-weight tower for $D_o \approx 20$ inches is selected from Figure 32, then Figure 31 suggests that an equivalent truss tower would have a radius between approximately 40 and 60 inches, depending upon the truss element diameter. These truss radii were judged to be too large because of blade consumption near the tower axis, wind drag and tower shadow effects, and unsightliness. Therefore, the 17-m turbine will have a tubular tower of approximately 20-inch outside diameter.

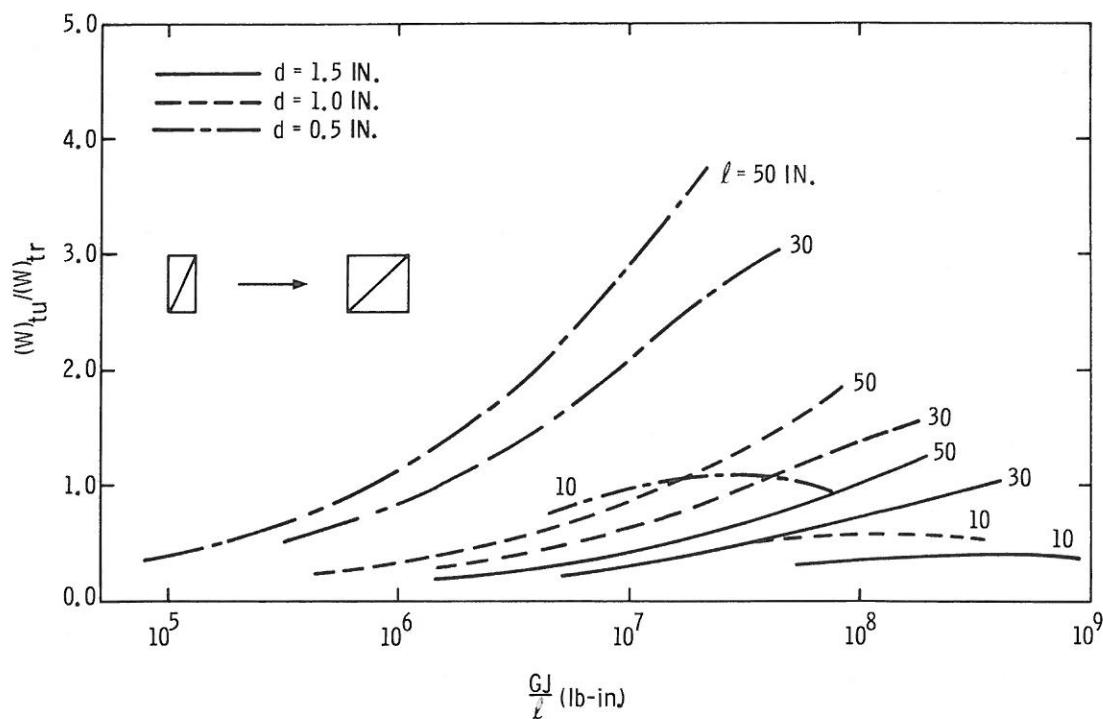


Figure 30. Ratio of the Weights of Tubular and Truss Towers Which Have Equivalent Torsional Stiffnesses

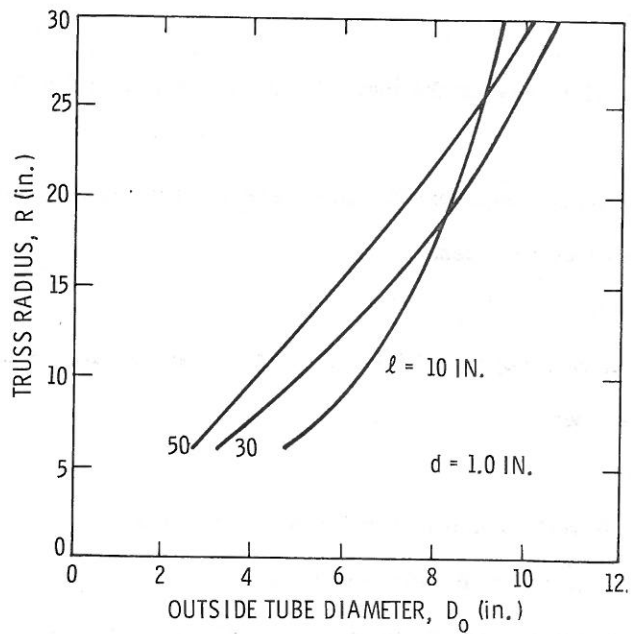


Figure 31. Relationship Between the Geometries of Tubular and Truss Tower Which Have Equivalent Torsional Stiffnesses

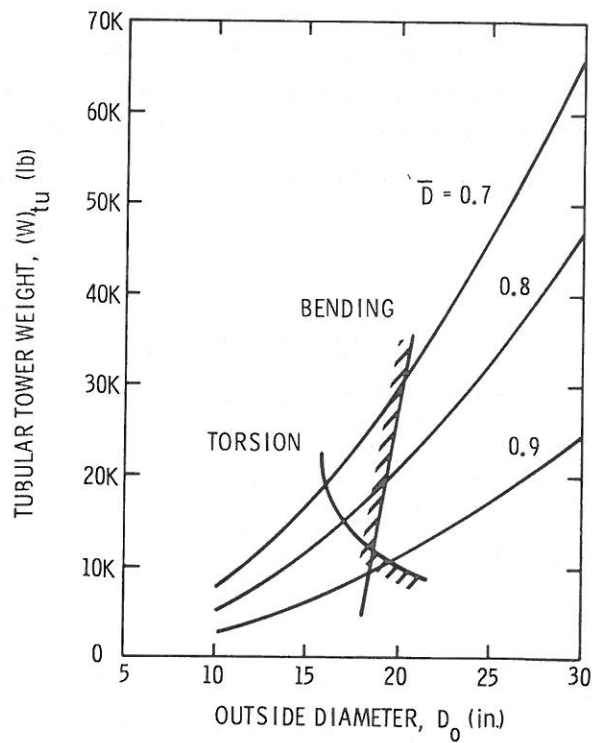


Figure 32. Minimum Weight Design Curves for Tubular Towers

Mechanical Design

The Sandia responsibilities for the mechanical components of the 17-m VAWT include the following:

1. The base support for mounting the base tower, the motor, and the generator.
2. The guy cable tiedown bases.
3. The base tower.
4. The base tower bearing mount for the rotating blade shaft and the bearings.
5. The braking system.
6. The blade shaft.
7. The blade shaft to the generator and motor drive train.
8. The blade hub mounts on the blade shaft.
9. The guy cable bearings and mount at the top of the blade shaft.
10. The guy cables.
11. The VAWT assembly.
12. The power train.

The base unit below the blade attachment contains the base tower, the axial and radial support for the VAWT, two flexible couplings, a torque sensor, a speed increaser, a right angle gear drive, a toothed pulley, a toothed belt, another toothed pulley, two more flexible couplings, a torque sensor, a synchronous generator, a clutch, and a starting motor. A schematic layout of the base is shown in Figure 33.

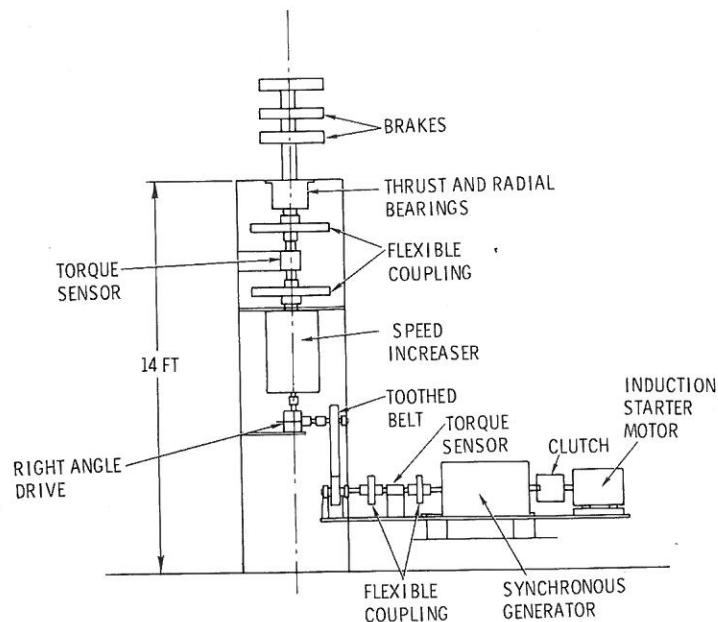


Figure 33. Turbine Base Design Schematic

The right-angle gear drive allows installation of the generator and motor on a horizontal axis. The arrangement not only permits easy access to these components for assembly or exchange due to design changes at a later time but also permits a shorter base tower than would be possible if the components were to be mounted on the vertical axis.

The toothed pulleys and belt permit further speed ratio changes. The right-angle gear drive and toothed pulleys and belt would probably not be designed into a production VAWT, but constitute a practical design for the desired flexibility in a research machine. A production VAWT would probably have a direct drive train to achieve maximum efficiency.

The flexible couplings are designed into the drive train on both sides of the torque sensors to protect the latter from possible shocks from the shafts. The flexible couplings also compensate for radial and angular misalignment between separately mounted components. One torque sensor is located at the turbine output shaft and one is located behind all the speed-increasing mechanisms and in front of the generator so the efficiency of the speed-increasing mechanisms can be measured. Both torque sensors are manufactured by Lebow Associates, Inc., and are of the strain-gage type.

A thrust bearing located at the top of the base tower supports the blade shaft, the blades, the guy cable loads, and related hardware. Another bearing is located below the thrust bearing to provide support structure stiffness and to maintain alignment of the shaft.

The same bearing design is repeated at the top of the blade shaft at the guy cable attachment. A radial bearing is located on the shaft above the thrust bearing to prevent a twisting load on the thrust bearing. The guy cables are attached as close to the top bearings as practical to provide the smallest moment arm and in turn the smallest bearing load due to any shaft misalignment. A load cell and adjustable turnbuckle will be a permanent part of each of the guy cables to provide a method of establishing cable tension and of adjusting cable tension to whatever tension is required.

The base tower is a structural steel angle welded structure, which is bolted to the concrete base. The steel braces are welded to three sides of the tower, with the fourth side bolted to the tower, to achieve access under the tower for possible replacement of power train components. The tower, which is 11 feet tall, tapers from an 8-foot square at the base to a 2-foot square at the top.

Assembly -- The assembly procedures will begin with the pouring of the concrete base support and the guy cable tiedown bases. The base tower will be placed on the concrete base and bolted into position at the four leg positions. The bottom shaft and the thrust and radial bearings will be bolted into position on the base tower. The bolts holding the base tower to the concrete base will be loosened and the bottom end of the base tower will be shimmed until the bottom shaft is vertical about its center of rotation and the base tower bolts are again tightened. This establishes a perpendicular centerline of rotation for the VAWT as well as for the power train under the shaft to the right-angle gear box.

The speed increaser, which will be bolted to its tower and placed under the bottom shaft, will be aligned so that the input shaft of the speed increaser is in line with the bottom shaft and secured to the concrete base. The shaft of the right-angle gear box will be aligned under the output shaft of the speed increaser in the same manner and secured to the concrete base.

Installation of the flexible couplings and torque sensor between the bottom shaft and the speed increaser, along with installation of the flexible couplings, torque sensor, generator, clutch, and motor will complete the drive train.

After installation of the brake calipers and brake power unit, the bottom part of the VAWT will be operational for checkout and a final check of perpendicularity of the bottom shaft.

The blade shaft will be assembled on top of the bottom shaft, and the guy cables will be assembled and properly tensioned. The blade shaft may now be powered by the motor. The final step will be the assembly of the blades to the blade shaft.

Low-Cost Blade Design

This effort is directed toward establishing several up-to-date Darrieus blade designs. It is intended that the resulting designs be considered target designs (especially in regard to costs) for those desiring to compete in this area. The emphasis has been on blades for the 17-m turbine; however, scale-up potential is also considered. The design(s) selected will depend on the number of blades expected to be produced.

The present in-house approach is to consider an overview of manufacturing processes and materials and to identify designs that appear to be economically attractive. These selected blade designs will then be refined by Sandia with the assistance of the appropriate manufacturing industry. Finally, a detailed design definition (drawings, procedures, etc) will be offered to competing manufacturers for a fabrication-only contract.

The fabrication-only-contract approach has two primary advantages:

- Details affecting blade design arise from an involvement and a familiarity with the entire Darrieus turbine program. It must be emphasized that the design of a Darrieus wind turbine blade is a highly interactive process and that the continuous updating of the design inputs encourages having both the input determination and the design activity within the same agency. The Darrieus turbine engineering activity is rapidly expanding, but the transfer of this technology is not instantaneous despite the honest and best efforts of the participants.
- Providing a completed blade design widens the pool of potential manufacturers (who may not possess the required analytical and engineering capabilities for a "turnkey" contract).

It is believed that this approach will be attractive to the many potential manufacturers who either do not have or cannot accumulate the various technical specialties required for the design of the blade. Furthermore, if given a specified production quantity along with the blade design, the manufacturer will establish the most accurate cost projection that can be made.

A preliminary study indicates the practicality of using either high-technology skills (e. g., automatic processing machinery) or low-technology skills (which are more labor intensive). However, it appears that the high-technology approach will probably yield the lowest cost blade. The nonrecurring costs for this approach will be high, therefore necessitating a very large production quantity. The blade designs are of metal monocoque (load-carrying skin) construction and involve such processes as automatic seam welding, roll forming, extrusion, investment casting, and stretch forming. The often-quoted goal of "\$2.00 per pound" does not appear out of reach.

After these high-technology designs (which appear to offer the lowest cost) have been solidified and projected costs have been firmly established, it is probable that these designs will be the economic "base-line" or target designs for following efforts.

Follow-on activities will include emphasis on the low-technology designs. Also, studies whereby industry can become more involved in the design process will be initiated.

The 5-m Turbine

Field Testing

The 5-m turbine (actually designed as, and previously designated as, a 15-foot-diameter unit) has recently undergone a series of operational field tests. This test series was initiated to determine whether field data could possibly be used to measure the performance of the 5-m turbine and to develop standardized techniques applicable for the 17-m test program.

The 5-m turbine was converted to operate at almost constant rpm by connecting a 1725-rpm induction motor to the turbine with a two-stage belt-type speed increaser. Through selection of various pulley diameters, a range of synchronous turbine speeds between 87.5 and 175 rpm is available. The turbine shaft torque is measured with a Lebow torsional variable differential transformer torquemeter located between the first and second transmission stages.

The constant-speed operation is desirable because the wind-applied torque on the blades can be equated to the measured shaft torque, avoiding the need to account for the angular acceleration of the turbine. Calculations have shown that failure to account for inertial effects due to "slip" in the induction motor (causing about a 1 percent rpm variation in the turbine as load changes) does not introduce unacceptable scatter in the results. Cup-type anemometers have been used for wind-velocity measurements. The most successful anemometer location, in terms of correlating output torque to windspeed, has been immediately upstream of the turbine and within two diameters of the machine. The "ideal" location remains to be found and is a subject of continuing investigation.

The overall objective is to measure windspeed and turbine torque and attempt to correlate these two variables. Anemometer readings taken from a weather tower about 300 feet from the turbine were used in initial test runs. It was found, however, that the direct correlation between measured torque and windspeed was very weak or nonexistent. The situation visibly improved when the anemometer was moved to a close-in (two turbine diameters) upstream location. However, simply plotting windspeed and torque points taken every 0.5 second* still yielded very scattered results (Figure 34). Although a smoothing technique consisting of averaging torque and windspeed over a 5-second interval improved the situation considerably, the data still exhibit much uncertainty. The averaged data, shown in Figures 35 and 36, indicate a definite trend that appears to be repeatable for the two different windspeed distributions shown.

*The time interval selected was based on an estimate of the best frequency response of the turbine and instrumentation.

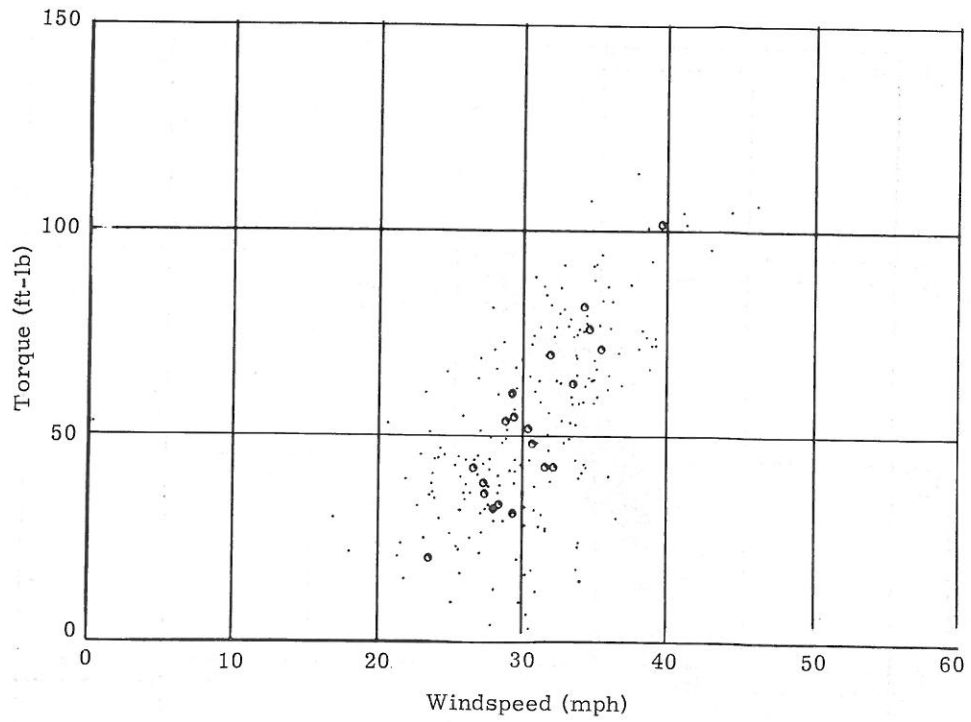


Figure 34. Pointwise Torque and Velocity Data (175-rpm) Sampled at 0.5-Second Intervals. Circular Points Are for 5-Second Averages

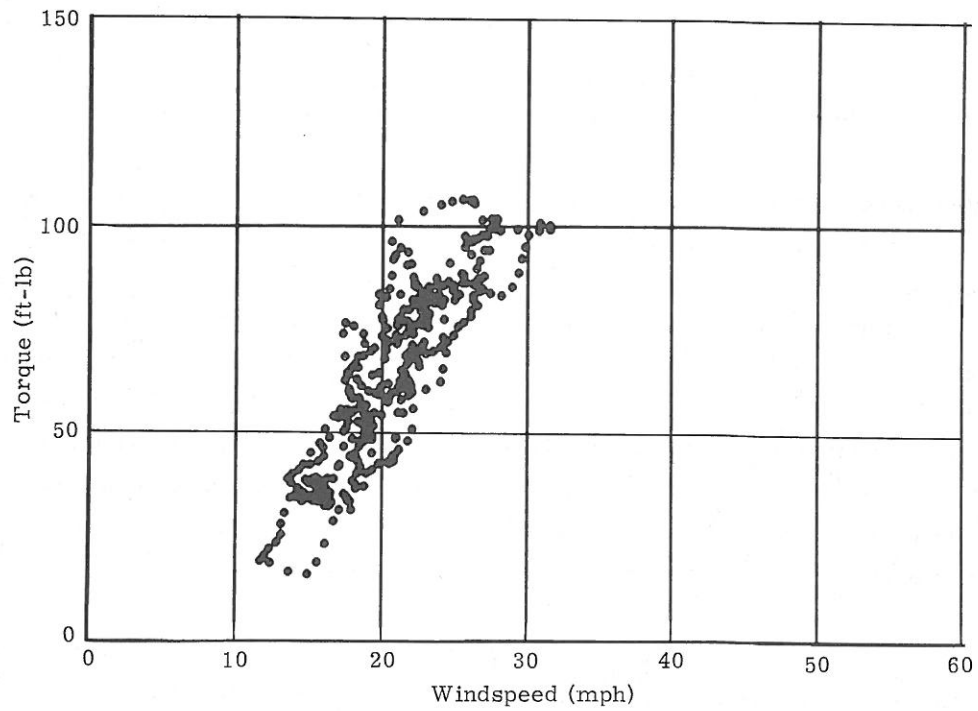


Figure 35. Five-Second Averaged Data. Approximately 3 Minutes of Data (175-rpm)

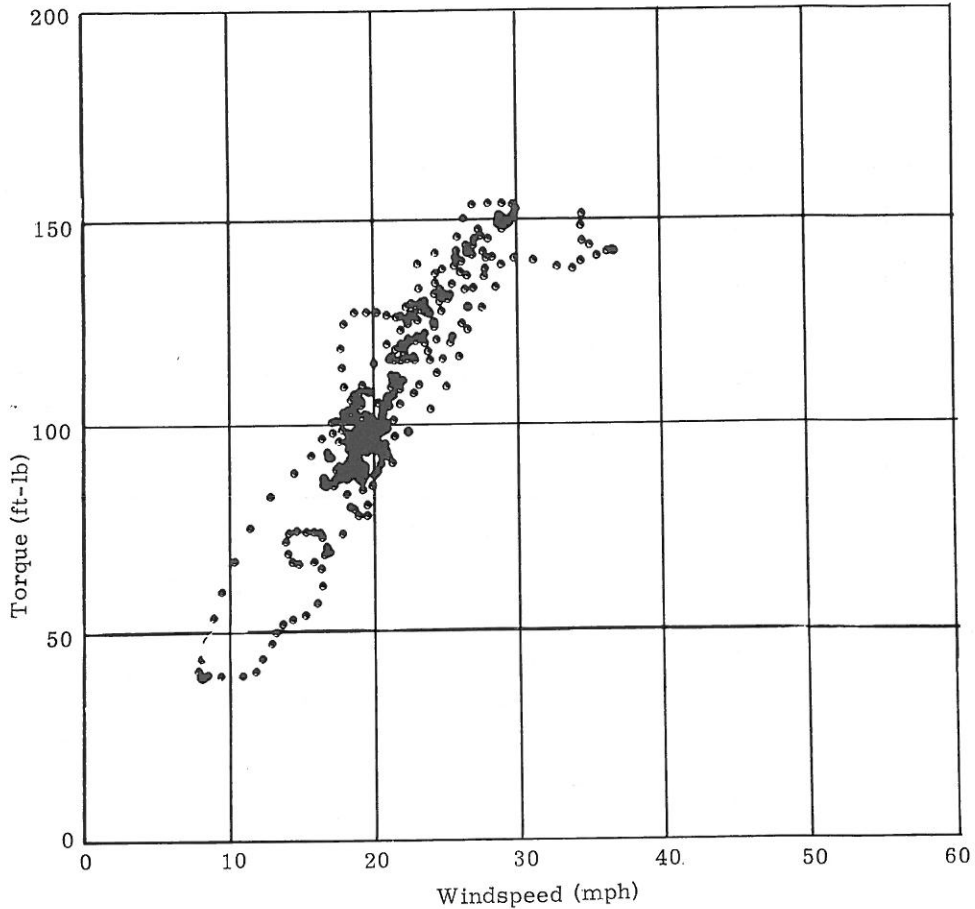


Figure 36. Repeatability Test. Same Configuration as Figure 35 With a Different Windspeed Record

Another scheme, the "method of bins," has received most of our attention because it has the advantage of indicating the velocity distribution associated with the wind record during the test. In this method, the velocity is divided into discrete bins of equal width, normally taken to be 2 mph. Each data pair (velocity and torque) is assigned to a bin associated with the velocity, and the corresponding torque is averaged with values previously accumulated in the bin. By keeping track of the number of points in each bin, the velocity distribution may be calculated. Typical results from this technique are shown in Figure 37 for a 175-rpm operating condition generated from about 3 minutes of data sampled at 0.5-second intervals. Results for an expanded data base taken over several different days lead to the even smoother results of Figure 38 for a 150-rpm operation. This curve was constructed from a total running time of ~ 30 minutes.

The effect of rpm variations is shown clearly in Figure 39 where there is a pronounced increase in output with increasing rpm, as is expected for turbines of this type.

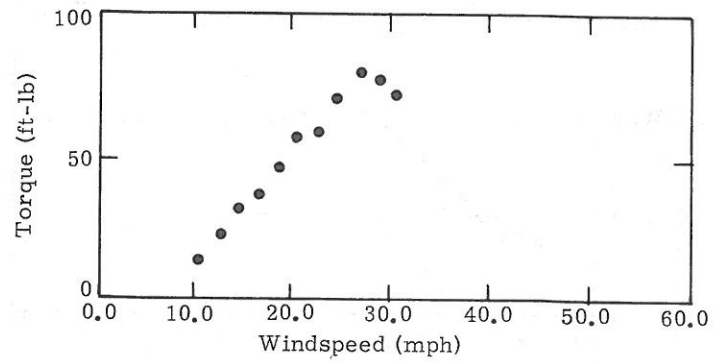
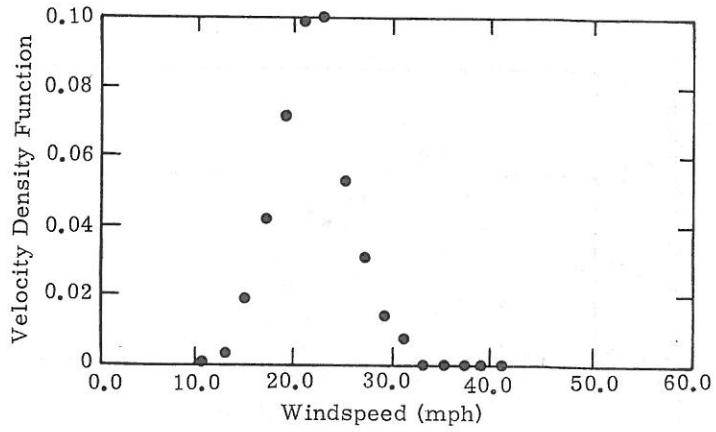


Figure 37. Method of Bins, Showing the Velocity Distribution (upper points) and Torque vs. Velocity for 175-rpm Operations

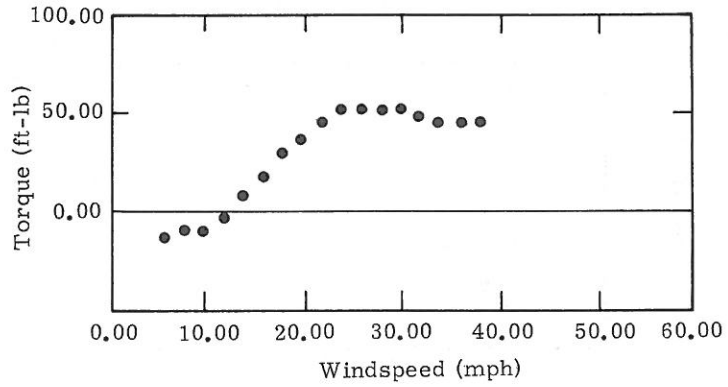
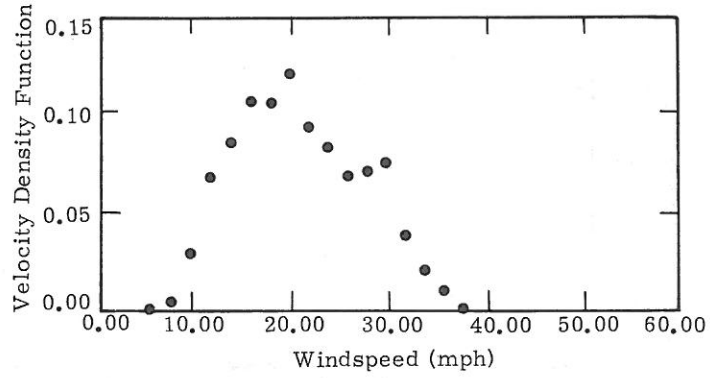


Figure 38. Method of Bins With an Expanded Velocity Distribution for 150-rpm Operations

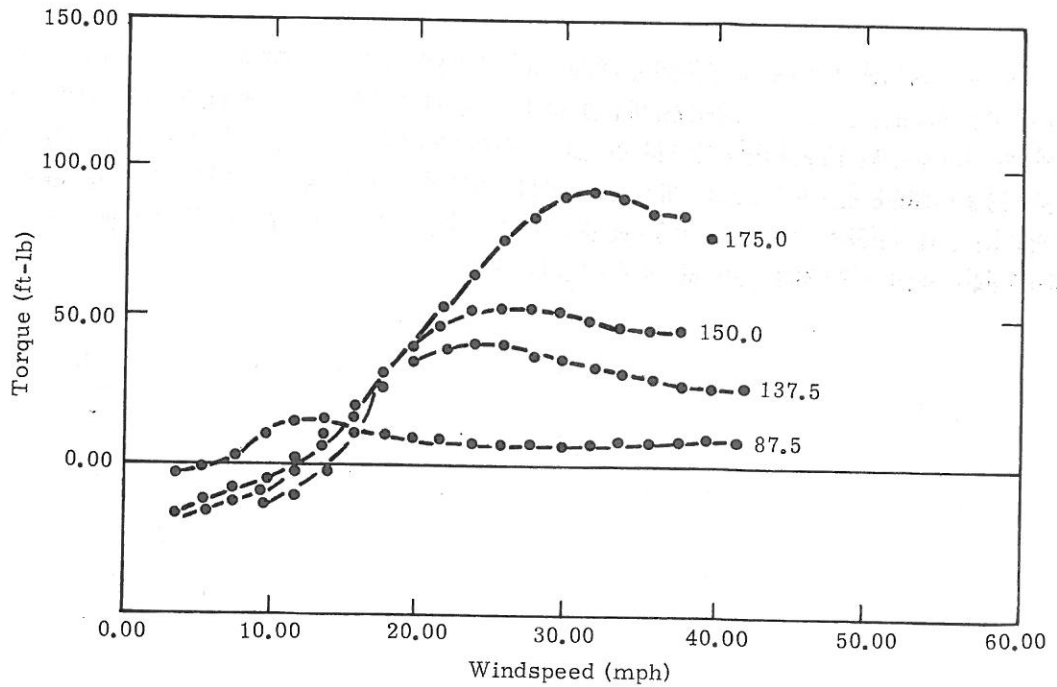


Figure 39. Families of Torque vs. Windspeed Responses
Showing the Effect of rpm on Turbine Output

The C_p curve may be readily derived from the torque data; however, uncertainties in velocity measurements tend to be amplified by the necessity to cube the velocity in the calculation. The peak C_p (Figure 40) for the 150-rpm data is much lower than anticipated (about 0.25). This effect is due either to poor aerodynamic performance of this particular turbine, systematic errors in the measurement process, or both, and will be investigated in greater detail in the upcoming quarter.

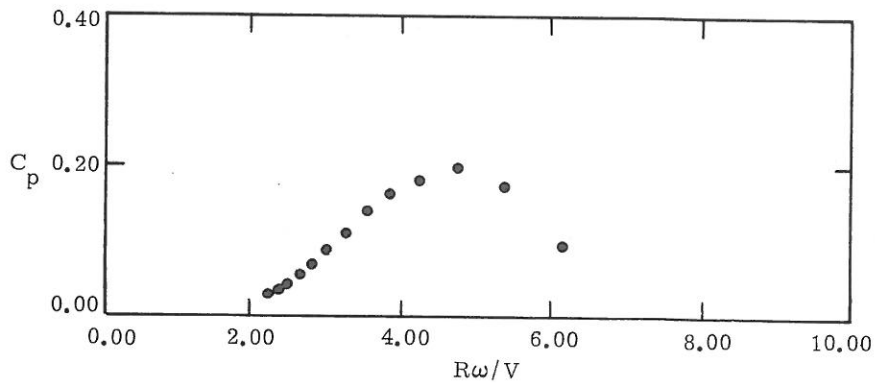


Figure 40. Power Coefficient Calculated From the 150-rpm
Data of Figure 38

The method of bins can produce a repeatable measure of turbine performance that is at least qualitatively accurate. More refinement is needed in understanding anemometer placement and data sampling procedures to put this technique on a firmer foundation. Data taken in the field should be applied to a turbine that has also been wind tunnel tested so that the cumulative effect of uncertainties can be determined. Finally, the process should be automated at the site so that the lost time between data collection and analysis can be eliminated.

PREVIOUS SANDIA PUBLICATIONS AND
PRESENTATIONS

Sandia Publications

- SAND74-0071 Wind Energy Potential in New Mexico, J. W. Reed, R. C. Maydew, B. F. Blackwell, July 1974.
- SAND74-0100 Practical Approximations to a Troposkien by Straight-Line and Circular-Arc Segments, G. E. Reis, B. F. Blackwell, March 1975.
- SAND74-0105 An Electrical System for Extracting Maximum Power from the Wind, A. F. Veneruso, December 1974.
- SLA-74-0154 Blade Shape for a Troposkien Type of Vertical-Axis Wind Turbine, B. F. Blackwell, G. E. Reis, April 1974.
- SLA-74-0160 The Vertical-Axis Wind Turbine - How it Works, B. F. Blackwell, April 1974.
- SAND74-0177 Some Geometrical Aspects of Troposkiens as Applied to Vertical-Axis Wind Turbines, B. F. Blackwell, G. E. Reis, March 1975.
- SLA-74-0298 A Wind-Powered Fresh Water Condensation Air Conditioning, Mariculture, and Aquiculture Integrated System for Pacific Atolls, D. B. Shuster, V. L. Dugan, R. H. Richards, June 1974.
- SAND74-0348 Wind Power Climatology of the United States, J. W. Reed, May 1975.
- SAND74-0378 Nonlinear Stress Analysis of Vertical-Axis Wind Turbine Blades, L. I. Weingarten, R. E. Nickell, April 1975.
- SAND74-0379 An Investigation of Rotation-Induced Stresses of Straight and of Curved Vertical-Axis Wind Turbine Blades, L. V. Feltz, B. F. Blackwell, March 1975.
- SAND74-0435 Wind Power Climatology, J. W. Reed, December 1974.
- SAND75-0165 Application of the Darrieus Vertical-Axis Wind Turbine to Synchronous Electrical Power Generation, J. F. Banas, E. G. Kadlec, W. N. Sullivan, March 1975.
- SAND75-0166 Wind Energy - A Revitalized Pursuit, B. F. Blackwell, L. V. Feltz, March 1975.
- SAND75-0204 Methods for Performance Evaluation of Synchronous Power Systems Utilizing the Darrieus Vertical-Axis Wind Turbine, J. F. Banas, E. G. Kadlec, W. N. Sullivan, April 1975.
- SAND75-0431 The Darrieus Turbine: A Performance Prediction Model Using Multiple Streamtubes, J. H. Strickland, October 1975.
- SAND75-0530 Engineering of Wind Energy Systems, J. F. Banas, W. N. Sullivan, January 1976.
- SAND76-0130 Wind Tunnel Performance Data for the Darrieus Wind Turbine with NACA-0012 Blades, B. F. Blackwell, L. V. Feltz, R. E. Sheldahl, to be published.
- SAND76-0131 Wind Tunnel Performance Data for Two- and Three-Cup Savonius Rotors, B. F. Blackwell, L. V. Feltz, R. E. Sheldahl, to be published.

External Publications

- U. S. Patent Number 3,918,839, "Wind Turbine," 16 Claims, B. F. Blackwell, L. V. Feltz, R. C. Maydew, November 11, 1975.
- J. W. Reed, "Wind Power Climatology," Weatherwise, 27, 6, December 1974, and SAND74-0435, Sandia Laboratories, December 1974.
- J. W. Reed, R. C. Maydew, and B. F. Blackwell, A Report of the Governor's Select Committee on Wind Energy, "Wind Energy Potential in New Mexico," Santa Fe, NM, June 7, 1975.
- L. I. Weingarten and R. E. Nickell, "Nonlinear Stress Analysis of Vertical-Axis Wind Turbine Blades," Journal of Engineering for Industry, Transactions ASME, Vol. 97, Series B, No. 4, November 1975, pp. 1234-1237.

Presentations

- J. W. Reed, "Some Notes on Wind Power Climatology," American Meteorological Society Climatology Conference, Asheville, NC, October 8-11, 1974.
- L. V. Feltz, "Wind Power - A Revitalized Pursuit," Heights Lions Club, Albuquerque, NM February 13, 1975.
- B. F. Blackwell, "Wind Energy - A Revitalized Pursuit," ASME Resource Recovery Symposium, Albuquerque, NM, March 6-7, 1975.
- R. C. Maydew, "Wind Energy," New Mexico State University, Las Cruces, NM, March 14, 1975.
- L. V. Feltz, "Wind Power - A Revitalized Pursuit," Sierra Club, University of Colorado, Boulder, CO, March 22, 1975.
- J. W. Reed, "Wind Energy Potential in the Southwest," Southwestern Technology Utilization Conference, Albuquerque, NM, April 16-17, 1975.
- L. V. Feltz, "Wind Power - A Revitalized Pursuit," New Mexico IEEE Spring Symposium on Energy Research in New Mexico, Albuquerque, NM, April 17-18, 1975.
- J. W. Reed, "Wind Power Climatology," New Mexico IEEE Spring Symposium on Energy Research in New Mexico, Albuquerque, NM, April 17-18, 1975.
- J. W. Reed, "Wind Power Climatology Research at Sandia Laboratories," 51st Annual American Association for the Advancement of Science Southwestern Division Meeting, Energy Resources Symposium, Los Alamos, NM, April 23-26, 1975.
- R. H. Braasch, "Power Generation with a Vertical Axis Wind Turbine," Wind Workshop II, Washington, DC, June 9-11, 1975.
- J. W. Reed, "Wind Climatology," ERDA-NSF Wind Energy Conversion Symposium Workshop, Washington, DC, June 9-11, 1975.
- J. W. Reed and B. F. Blackwell, "Some Climatological Estimates of Wind Power Availability," 2nd U.S. National Conference on Wind Engineering Research, Ft. Collins, CO, June 23-25, 1975.
- B. F. Blackwell and G. E. Reis, "Geometrical Aspects of the Troposphere as Applied to the Darrieus Vertical-Axis Wind Turbine," ASME Paper 75-DET-42, ASME Design Engineering Technical Conference, Washington, DC, September 1975
- A. F. Veneruso, "VAWT Technology," New York Ocean Science Laboratory, Montauk, Long Island, NY, August 20, 1975.
- L. V. Feltz, "Wind Energy Potential," Bureau of Indian Affairs, Juneau, Alaska, September 11, 1975.
- A. F. Veneruso, "VAWT Technology," United Nations Office of Technical Cooperation, UN Hdqs, NY, September 25, 1975.
- L. I. Weingarten, "Nonlinear Stress Analysis of Vertical-Axis Wind Turbine Blades," ASME Paper 75-DET-35, ASME Design Engineering Technical Conference, Washington, DC, September 1975.
- R. C. Reuter, "Wind Power," Rio Grande Lions Club, Albuquerque, NM, October 10, 1975.
- E. G. Kadlec, "Sandia Wind Power Program," American Wind Energy Association, Santa Rosa, CA, October 11, 1975.
- E. G. Kadlec, "Sandia Wind Power Program," Iowa 2000 Conference, Ames, Iowa, October 12, 1975.
- A. F. Veneruso, "VAWT Technology and Electrical Considerations for Utilities," Public Service Company of NM, Albuquerque, NM, October 23, 1975
- L. I. Weingarten and L. V. Feltz, "Material and Manufacturing Considerations for the Vertical-Axis Wind Turbine," Seventh National Society for the Advancement of Material and Process Engineering Technical Conference, Albuquerque, NM, October 1975.
- E. G. Kadlec, "Sandia Wind Power Program," Industrial College of the Armed Forces, Albuquerque, NM, December 8, 1975.

REFERENCES

1. B. F. Blackwell, The Vertical-Axis Wind Turbine - How it Works, SLA-74-0160, April 1974.
2. B. F. Blackwell and L. V. Feltz, Wind Energy - A Revitalized Pursuit, SAND75-0166, March 1975.
3. J. F. Banas, E. G. Kadlec, and W. N. Sullivan, Application of the Darrieus Vertical-Axis Wind Turbine to Synchronous Electrical Power Generation, SAND75-0204, April 1975.
4. J. F. Banas, E. G. Kadlec, and W. N. Sullivan, Methods for Performance Evaluation of Synchronous Power Systems Utilizing the Darrieus Vertical-Axis Wind Turbine, SAND75-0165, April 1975.
5. J. H. Strickland, The Darrieus Turbine: A Performance Prediction Model Using Multiple Streamtubes, Sandia Laboratories, SAND-75-0431, October 1975.
6. P. South and R. S. Rangi, An Experimental Investigation of a 12-ft Diameter High Speed Vertical-Axis Wind Turbine, LTR-LA-166, National Research Council of Canada, April 1975.
7. J. F. Banas, W. N. Sullivan (editors), Sandia Vertical-Axis Wind Turbine Program Technical Quarterly Report, October-December 1975, SAND76-0036, April 1976.

DISTRIBUTION:

TID-4500-R64, UC-60 (249)

R. J. Templin
Low Speed Aerodynamics Section
NRC-National Aeronautical Establishment
Ottawa 7, Ontario, Canada K1A0R6

A. Robb
Memorial Univ. of Newfoundland
Faculty of Eng. & Applied Sciences
St. John's Newfoundland
Canada A1C 5S7

H. Sevier
Rocket and Space Division
Bristol Aerospace Ltd.
P. O. Box 874
Winnipeg, Manitoba
R3C 2S4 Canada

V. A. L. Chasteau
Department of Mech. Engineering
The University of Auckland
Private Bag
Auckland, New Zealand

G. Herrera
Jet Propulsion Lab
4800 Oak Grove Drive
Pasadena, CA 91103

NASA Langley Research Center
Hampton, VA 23365
Attn: R. Muraca, MS 317

NASA Lewis Research Center (2)
2100 Brookpark Road
Cleveland, OH 44135
Attn: J. Savino, MS 509-201
R. L. Thomas

ERDA Headquarters (20)
Washington, DC 20545
Attn: L. Divone
Chief, Wind Energy
Conversion Branch

University of New Mexico (2)
Albuquerque, NM 87131
Attn: K. T. Feldman
Energy Research Center
V. Sloglund
ME Department

A. V. da Rosa
Stanford Electronic Laboratories
Radio Science Laboratory
Stanford, CA 94305

A. N. L. Chiu
Wind Engineering Research Digest
Spalding Hall 357
University of Hawaii
Honolulu, HI 96822

R. N. Meroney
Colorado State University
Dept. of Civil Engineering
Fort Collins, CO 80521

A. G. Vacroux
Illinois Institute of Technology
Dept. of Electrical Engineering
Chicago, IL 60616

Oklahoma State University (2)
Stillwater, OK 74074
Attn: W. L. Hughes
EE Department
D. K. McLaughlin
ME Department

Oregon State University (2)
Corvallis, OR 97330
Attn: R. Wilson
ME Department
R. W. Thresher
ME Department

Texas Tech University (3)
Lubbock, TX 79409
Attn: K. C. Mehta, CE Dept.
J. Strickland, ME Dept.
J. Lawrence, ME Dept.

R. G. Watts
Tulane University
Dept. of Mechanical Engineering
New Orleans, LA 70018

Aero Engineering Department (2)
Wichita State University
Wichita, KS 67208
Attn: M. Snyder
Bill Wentz

Nevada Operations Office, ERDA (2)
P. O. Box 14100
Las Vegas, NV 89114
Attn: R. Ray, Operations
H. Mueller, ARL

Los Alamos Scientific Lab (7)
P. O. Box 1663
Los Alamos, NM 87544
Attn: R. R. Brownlee, J-9
J. R. Bartlit, Qu-26
J. D. Balcomb, Q-DO-T
R. G. Wagner, P-5
J. Nachamkin, T-DO-TEC
S. W. Depp, E-DO
H. Deinken, ADWP-1

DISTRIBUTION (cont):

ERDA/ALO (3)
Kirtland AFB East
Albuquerque, NM 87115
Attn: D. K. Knowlin
D. C. Graves
D. W. King

R. Camerero
Faculty of Applied Science
University of Sherbrooke
Sherbrooke, Quebec
Canada J1K 2R1

American Wind Energy Association
21243 Grand River
Detroit, MI 48219

E. E. Anderson
Dept. of Mechanical Engineering
South Dakota Sch. of Mines & Tech.
Rapid City, SD 57701

E. S. Takle
Climatology and Meteorology
312 Curtiss Hall
Iowa State University
Ames, IA 50011

P. B. S. Lissaman
Aeroenvironment, Inc.
660 South Arroyo Parkway
Pasadena, CA 991105

R. A. Parmelee
Department of Civil Engineering
Northwestern University
Evanston, IL 60201

J. Park
Helion
P. O. Box 4301
Sylmar, CA 91342

W. F. Foshag
Aerophysics Company
3500 Connecticut Avenue NW
Washington, DC 20008

W. L. Harris
Aero/Astro Department
MIT
Cambridge, MA 02139

K. Bergey
Aero Engineering Department
University of Oklahoma
Norman, OK 73069

J. Fischer
F. L. Smidth & Company A/S
Vigerslevalle 77
2500 Valby, Denmark

H. M. Busey
DMA, Safety and Facilities A-364
ERDA Headquarters
Washington, DC 20545

P. Bailey
P. O. Box 3
Kodiak, AK 99615

M. E. Beecher
Solar Energy Collection
Arizona State University
University Library
Tempe, AZ 85281

U. A. Coty
Lockheed - California Co.
Box 551-63A1
Burbank, CA 91520

Lawrence Livermore Laboratory (2)
P. O. Box 808 L-340
Livermore, CA 94550
Attn: D. W. Dorn
D. Hardy

J. A. Garate
General Electric
Valley Forge Space Center
King of Prussia, PA 19406

O. Krauss
Division of Engineering Research
Michigan State University
East Lansing, MI 48823

P. Calnan
Electrical Research Associates
Cleeve Road
Leatherhead
Surrey, England

V. Nelson
Department of Physics
West Texas State University
P. O. Box 248
Canyon, TX 79016

E. Gilmore
Amarillo College
Amarillo, TX 79100

DISTRIBUTION (cont)

L. Liljdahl
Building 303
Agriculture Research Center
USDA
Beltsville, MD 20705

T. Wentink, Jr.
Geophysical Institute
University of Alaska
Fairbanks, AK 99701

E. J. Warchol
Bonneville-Power Administration
P. O. Box 3621
Portland, OR 97225

D. Lindley
Mechanical Engineering
University of Canterbury
Christchurch, New Zealand

Olle Ljungstrom
Swedish Board for Tech. Development
FACK
S-100 72 Stockholm 43, Sweden

Robert Brulle
McDonnell-Douglas
P. O. Box 516
Dept. 241, Bldg. 32
St. Louis, MO 83166

R. Walters
W. Va. University
Aero Engineering
1062 Kountz Ave
Morgantown, WV 26505

Albert Fritzsche
Dornier System GmbH
Postfach 1360
7990 Friedrichshafen
West Germany

P. N. Shankar
Aerodynamics Division
National Aeronautical Laboratory
Bangalore 560017
India

Peter Andersen
Karstykke 42
Vvelse 3550
Slangerup, Denmark

Otto de Vries
National Aerospace Laboratory
Anthony Fokkerweg 2
Amsterdam 1017
The Netherlands

J. P. Johnston
Mechanical Engineering
Stanford University
Stanford, CA 94305

Lt T. Colburn
USCG R&D Center
Avory Point
Groton, CT 06340

James Meiggs
Kaman Sciences Corp.
P. O. Box 7463
Colorado Springs, CO 80933

G. P. Hawkins
Irwin Industries
6045 West 55th Place
Arvada, CO 80002

D. Greider
Solar Central
7213 Ridge Rd.
Mechanicsburg, OH 43044

D. G. Shepherd
Sibley School of Mechanical and
Aerospace Engineering
Cornell University
Ithaca, NY 14853

B. Maribo Pedersen
Dept of Fluid Mechanics
Bldg. 404, DTH
2800 Lyngby
Denmark

Leo H. Soderholm
Rm 213 Ag Engr.
Iowa Statue University
Ames, IA 50011

J. B. F. Scientific Corporation
2 Jewel Drive
Wilmington, MA 01887
Attn: E. E. Johanson

United Nations Environment Programme
485 Lexington Avenue
New York, NY 10017
Attn: I. H. Usmani

G. N. Monsson
Mineral Development Geologist
Dept. of Economic Planning and Development
Barrett Building
Cheyenne, WY 82002

DISTRIBUTION (cont):

Dr. O. Igra
Dept. of Mechanical Engineering
Ben-Gurion University of the Negev
Beer-Sheva, Israel

H. K. Skeele
Learning Unlimited Corporation
72 Park Street
New Canaan, CT 06840

A. J. Karalis, P.E.
Manager, Special Projects
Advanced Engineering Department
United Engineers and Constructors, Inc.
30 South 17th Street
Philadelphia, PA 19101

Piet Bos
Program Manager, Solar Energy
Electric Power Research Institute
3412 Hillview Avenue
Palo Alto, CA 94303

Professor Norman D. Ham
Massachusetts Institute of Technology
77 Massachusetts Avenue
Cambridge, MA 02139

J. Barzda
Chief of Systems Research
Kaman Aerospace Corporation
Old Windsor Road
Bloomfield, CT 06002

Southwest Research Institute (2)
P. O. Drawer 28510
San Antonio, TX 78284
Attn: W. L. Donaldson
Senior Vice President
R. K. Swanson

L. H. J. Maile
Engineering Manager
Dominion Aluminum Fabricating Ltd.
3570 Hawkestone Road
Mississauga, Ontario L5C 2V8 Canada

1000 G. A. Fowler
1200 W. A. Gardner
1280 T. B. Lane
1281 S. W. Key
1281 J. H. Biffle
1281 R. Rodeman
1284 R. T. Othmer
1284 W. N. Sullivan
1284 L. I. Weingarten
1300 D. B. Shuster
1320 M. L. Kramm
1324 E. C. Rightley
1324 L. V. Feltz
1324 D. F. McNeill
1330 R. C. Maydew
1333 S. McAlees, Jr.

1333 B. F. Blackwell
1333 R. E. Sheldahl
1400 A. Y. Pope
3161 J. E. Mitchell (50)
5000 A. Narath
5431 D. W. Lobitz
5443 J. W. Reed
5700 J. H. Scott
5710 G. E. Brandvold
5715 R. H. Braasch
5715 E. G. Kadlec (100)
5715 C. E. Longfellow
5715 R. C. Reuter
5715 R. S. Rusk
5715 A. F. Veneruso
5740 V. L. Dugan
5742 S. G. Varnado
5742 J. F. Banas
8000 T. B. Cook, Jr.
8100 L. Gutierrez
8110 A. N. Blackwell
8300 B. F. Murphey
8320 T. S. Gold
9622 R. C. Anderson
9743 K. G. Grant
8266 E. A. Aas (2)
3141 C. A. Pepmueller (Actg.) (5)
3151 W. L. Garner (3)
For ERDA/TIC (Unlimited Release)
ERDA/TIC (25)
(R. P. Campbell, 3171-1)

Reprinted January 1980

